What we have learned from geoneutrinos (2005–2020)?



Ondřej Šrámek

Department of Geophysics,
Charles University, Prague, Czech Republic
ondrej.sramek@gmail.com



GAČR
GRANTOVÁ AGENTURA ČESKÉ REPUBLIKY

Collaboration with: Bill McDonough, Bedřich Roskovec, Scott Wipperfurth, Yufei Xi, …

Presented on 2 December 2020 at "Geodynamický seminář" of Department of Geophysics, Charles University

Space Sci Rev (2020) 216:37
https://doi.org/10.1007/s11214-020-00656-z

Check for updates

On the Distribution and Variation of Radioactive Heat Producing Elements Within Meteorites, the Earth, and Planets

C. O'Neill[1] · H.S.C. O'Neill[1] · A.M. Jellinek[1]

Received: 1 October 2019 / Accepted: 5 March 2020
© Springer Nature B.V. 2020

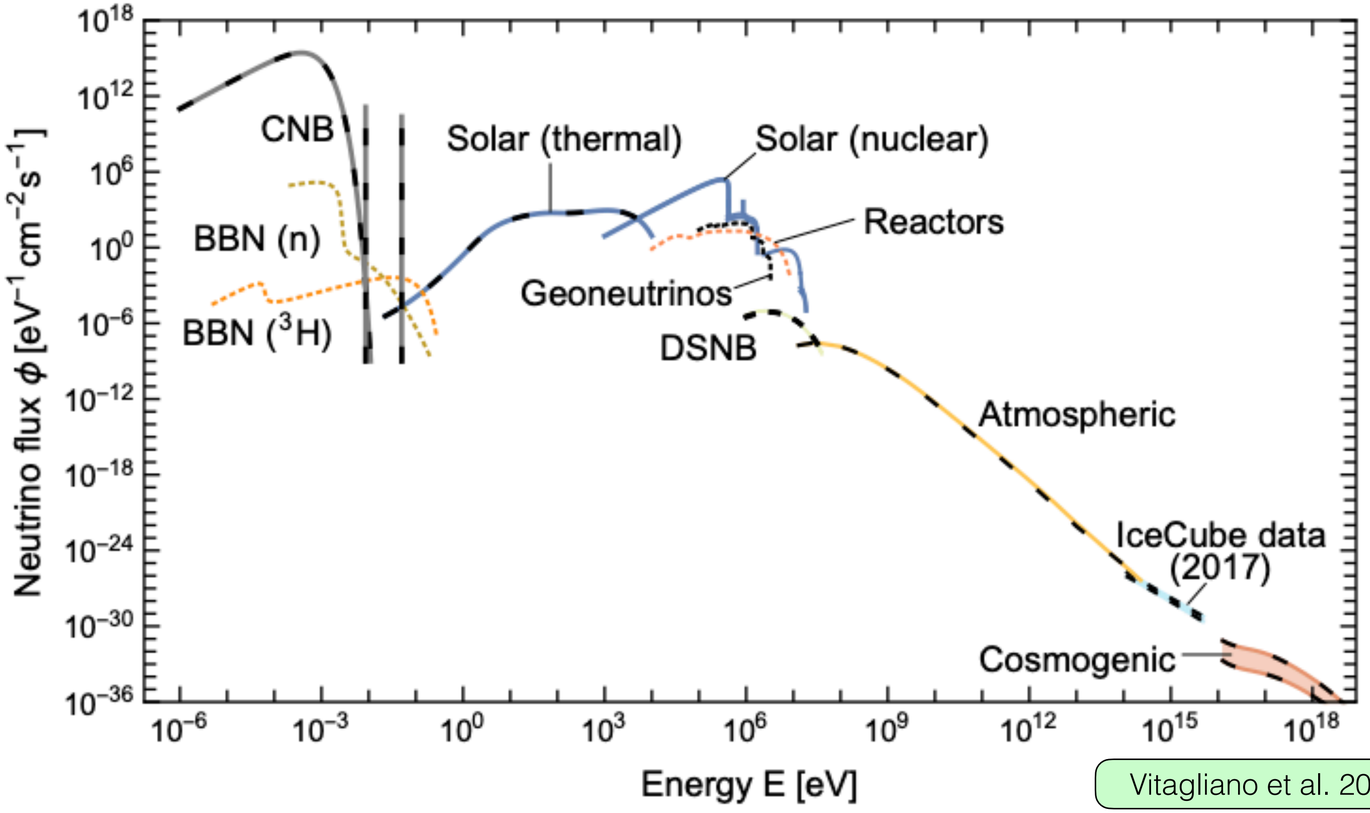
4 Earth's HPE abundance

Earth's internal heat production budget can be estimated in a number of ways. There is a geodynamic approach, using Earth's total heat loss and assuming an energy budget to constrain heat production, and element ratios to constrain HPE concentrations (Turcotte and Schubert 2002). The geochemical approach utilises either direct measurements (including chondrites), and considers partitioning of HPEs into different reservoirs to constrain element concentrations (O'Neill 2016). And more recently, emerging geoneutrino measurements have been able to provide a direct measurement of the concentration (and eventually, the distribution) of HPEs in the Earth's interior.

Although argued by Agostini et al. (2019) to be marginally consistent with a geodynamic model for mantle heat generation, these values are not consistent with published chondritic or non-chondritic BSE compositions (Table 4). In particular, these results exclude the enstatite-chondrite or non-chondritic Earth models at a high degree of confidence and, thus, more work is required before geoneutrino constraints can be regarded as reliable.

Are geoneutrinos useful?

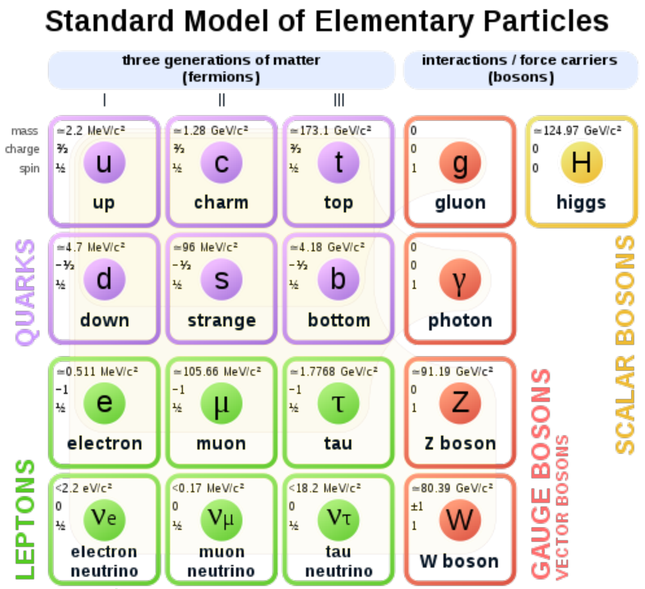
The broad spectrum of neutrinos around us

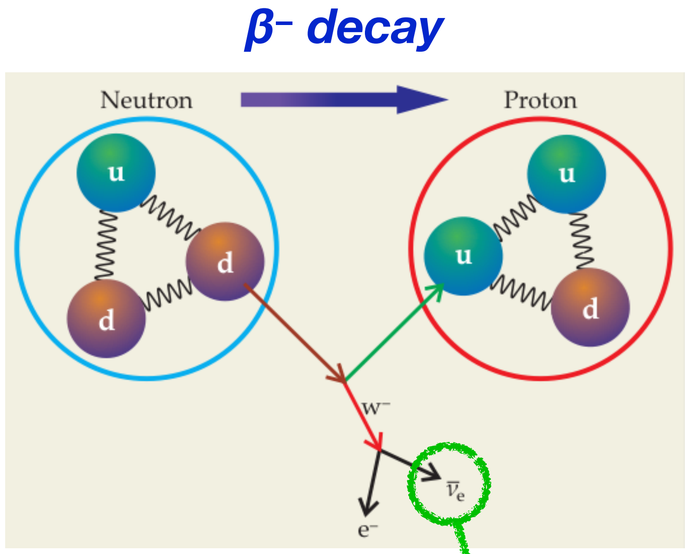


Vitagliano et al. 2019 arXiv:1910.11878

“Grand Unified Neutrino Spectrum” (GUNS) at Earth

Neutrinos





Geoneutrinos

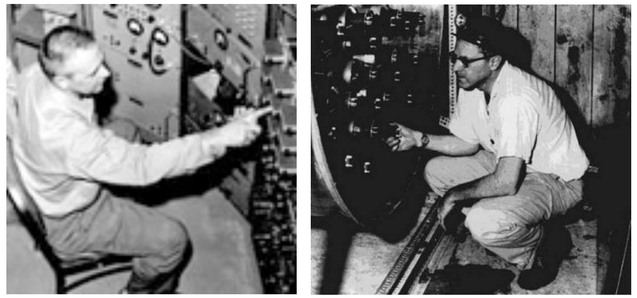
Electron antineutrinos and neutrinos emitted in β decays (β⁻, β⁺, EC) of naturally occurring radionuclides (mostly from ^{40}K, ^{232}Th, ^{238}U).

Brief (geo)neutrino history



1930: Pauli proposes a new neutral particle to resolve energy conservation problem in β^- decay

1956: Reines & Cowan reported the first electron antineutrino detection (reactor antineutrinos)





NATURE VOL. 310 19 JULY 1984 — REVIEW ARTICLE — 191

Antineutrino astronomy and geophysics

Lawrence M. Krauss*, Sheldon L. Glashow† & David N. Schramm‡

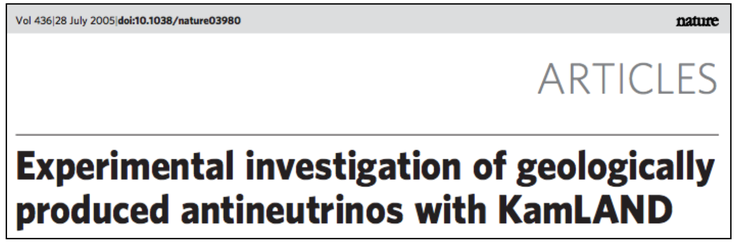
* Lyman Laboratory of Physics, Harvard University, Cambridge, Massachusetts 02138, USA
† Department of Physics, Boston University, Boston, Massachusetts 02215, USA
‡ Department of Physics and Astrophysics, Enrico Fermi Institute, University of Chicago, Chicago, Illinois 60637, USA

Radioactive decays inside the Earth produce antineutrinos that may be detectable at the surface. Their flux and spectrum contain important geophysical information. New detectors need to be developed, discriminating between sources of antineutrinos, including the cosmic-background. The latter can be related to the frequency of supernovas.

1984: Krauss, Glashow, Schramm:
Antineutrino astronomy and geophysics

2005: first reported measurement of geoneutrinos by KamLAND experiment

2010: measurement reported by Borexino experiment



Vol 436|28 July 2005|doi:10.1038/nature03980 nature

ARTICLES

Experimental investigation of geologically produced antineutrinos with KamLAND

Geoneutrinos

- Radionuclides in the Earth:

$$^{238}_{92}\mathrm{U} \longrightarrow {}^{206}_{82}\mathrm{Pb} + 8\alpha + 6\mathrm{e}^- + 6\bar{\nu}_e + 51.689\ \mathrm{MeV}$$

$$^{235}_{92}\mathrm{U} \longrightarrow {}^{207}_{82}\mathrm{Pb} + 7\alpha + 7\mathrm{e}^- + 7\bar{\nu}_e + 46.402\ \mathrm{MeV}$$

$$^{232}_{90}\mathrm{Th} \longrightarrow {}^{208}_{82}\mathrm{Pb} + 6\alpha + 4\mathrm{e}^- + 4\bar{\nu}_e + 42.652\ \mathrm{MeV}$$

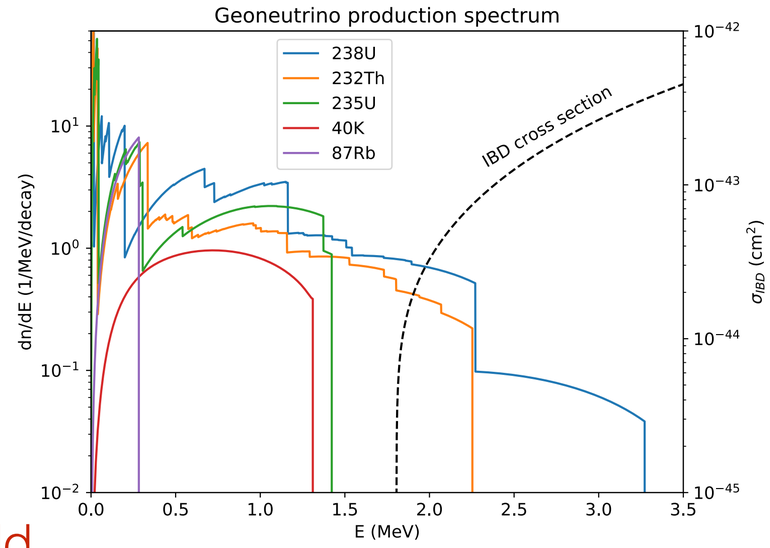
$$^{40}_{19}\mathrm{K} \xrightarrow{89.3\%} {}^{40}_{20}\mathrm{Ca} + \mathrm{e}^- + \bar{\nu}_e + 1.311\ \mathrm{MeV}$$

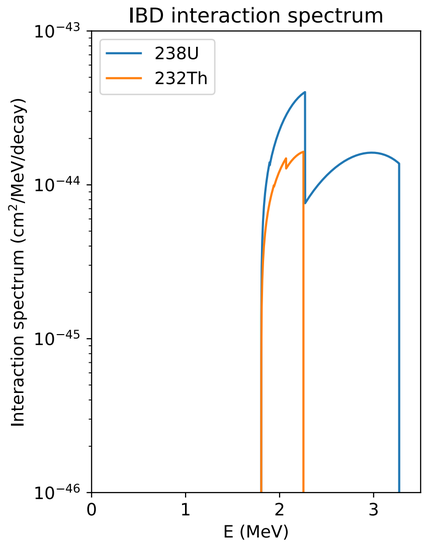
$$^{40}_{19}\mathrm{K} + \mathrm{e}^- \xrightarrow{10.7\%} {}^{40}_{18}\mathrm{Ar} + \nu_e + 1.505\ \mathrm{MeV}$$

Geoneutrinos:
Mostly electron antineutrinos

Measuring radiogenic power in the Earth

Energy per decay chain
Part carried away by geoneutrinos
Rest is converted to heat





Geoneutrino energy above IBD threshold

$$\bar{\nu}_e + p \rightarrow e^+ + n$$

How are geoneutrinos detected?

Inverse beta decay reaction

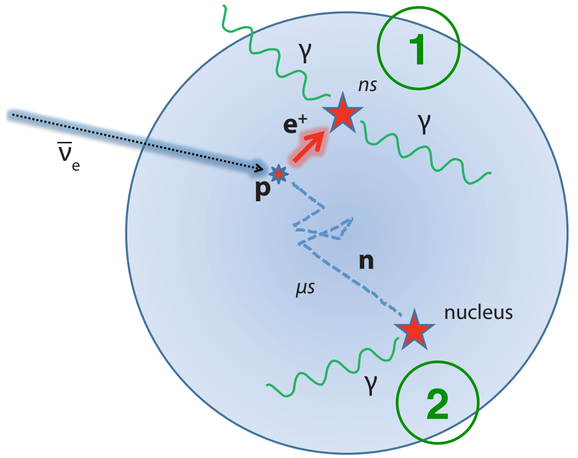
Energy threshold 1.8 MeV

only highest energy antineutrinos ^{232}Th and ^{238}U

Small interaction cross section

~10^{-44} cm^2 for ~1 MeV

$$\bar{\nu}_e + p \rightarrow e^+ + n$$

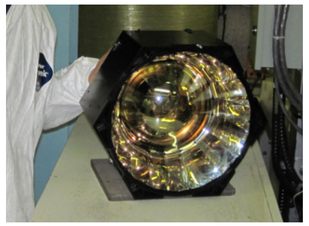


Liquid scintillator detectors:

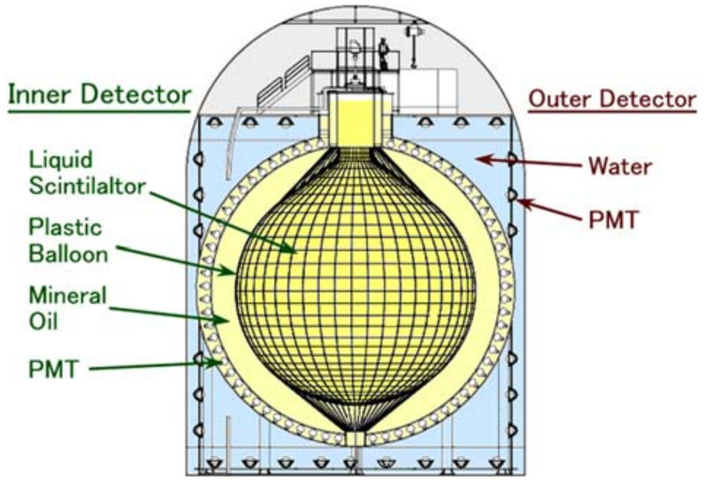
Large ~10^{32} free protons or ~1 kiloton of scintillator

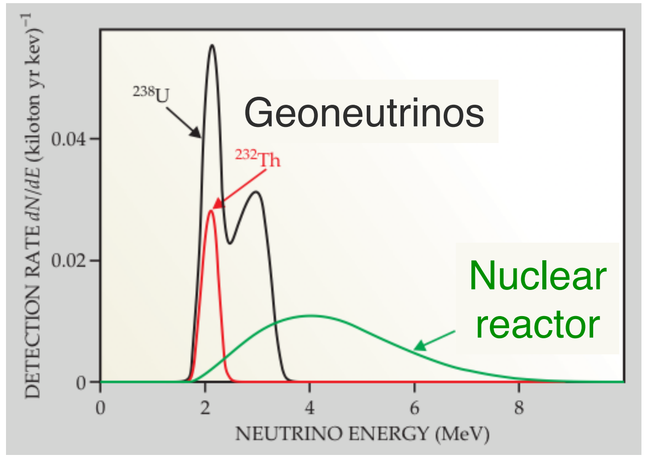
Underground to shield from muon background

Double-flash coincidence

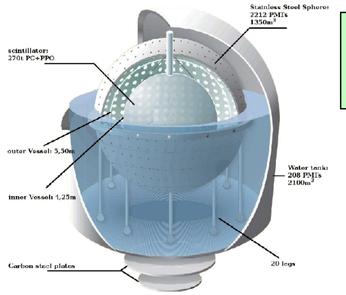








Geoneutrino detectors

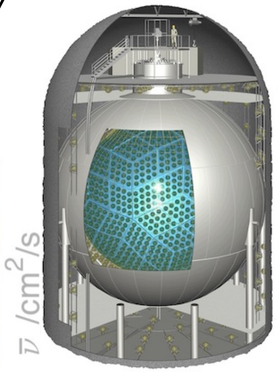


Borexino

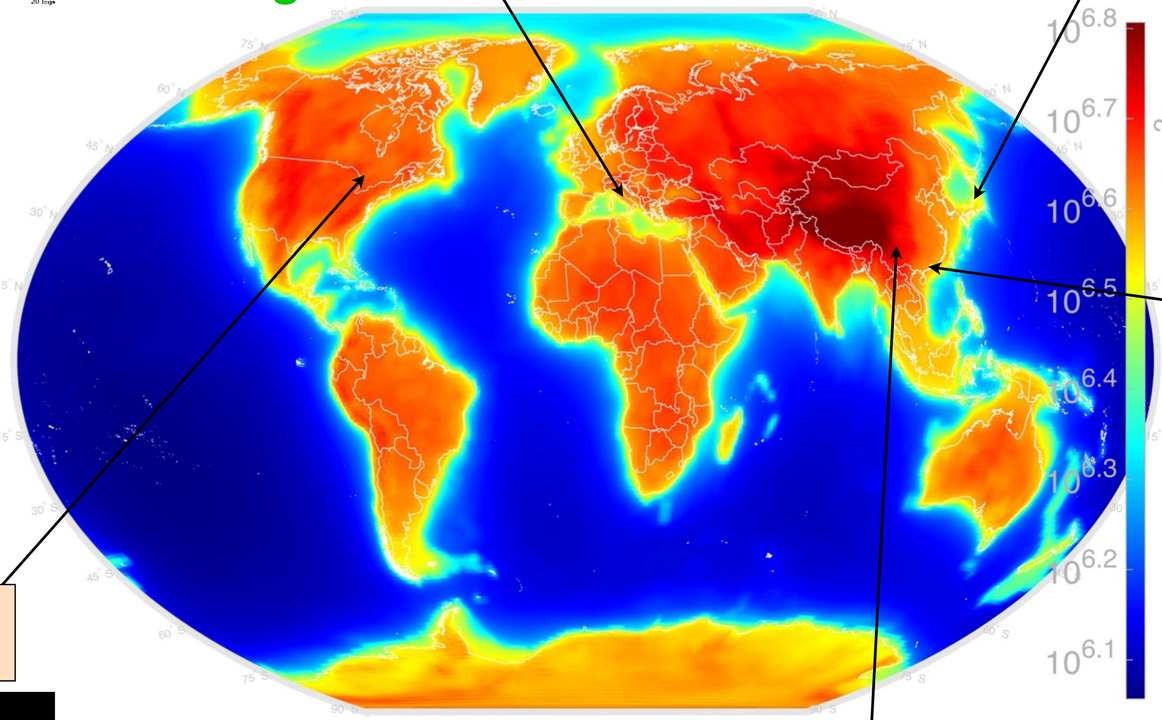
0.3 kton
3.7 km.w.e.
running

Large (~1 kton) underground liquid scintillator detectors

KamLAND

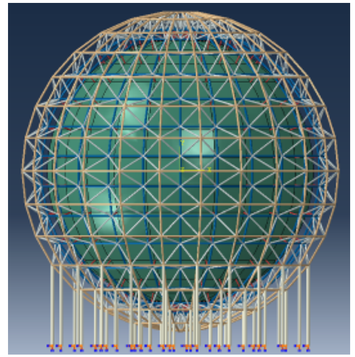


1 kton
2.7 km.w.e.
running

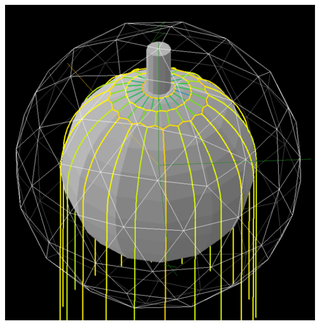


JUNO

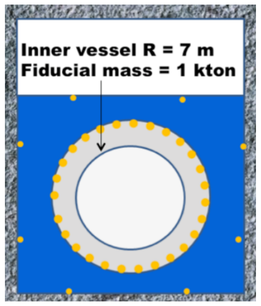
20 kton
1.5 km.w.e.
under constr.
(2020)



SNO+



1 kton
5.4 km.w.e.
expected online soon

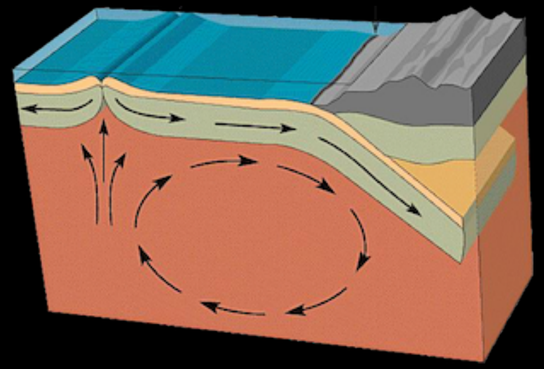


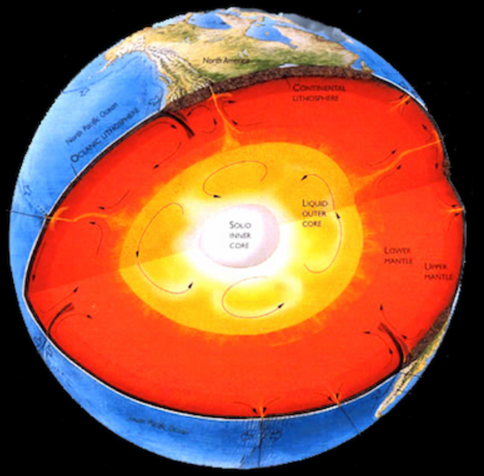
Jinping

4 kton
6.7 km.w.e.
R&D

How much radiogenic power in this planet…

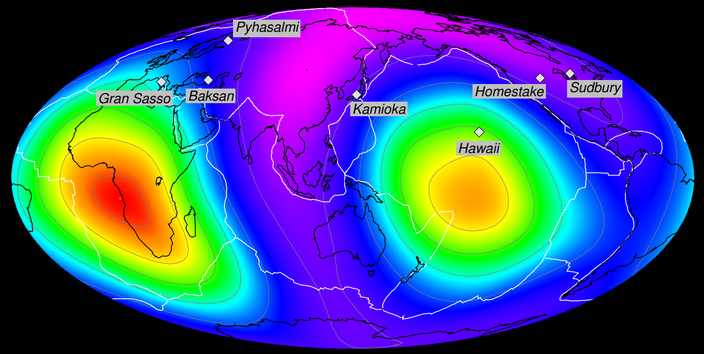


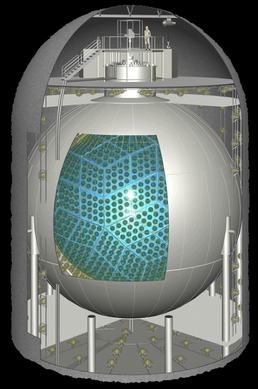




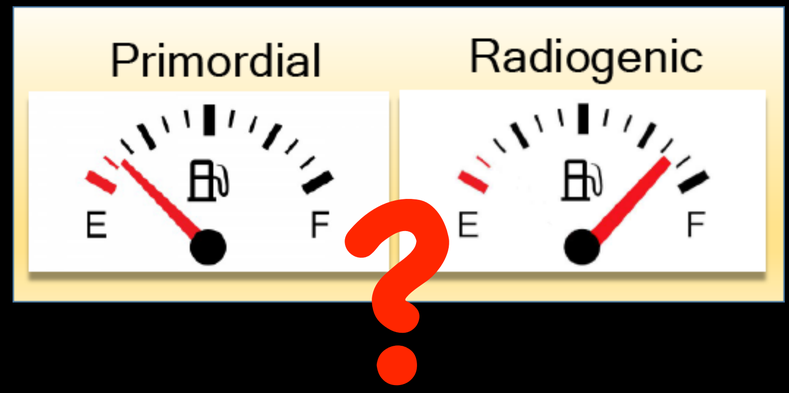
…to drive Earth's dynamics?

Geoneutrino detection

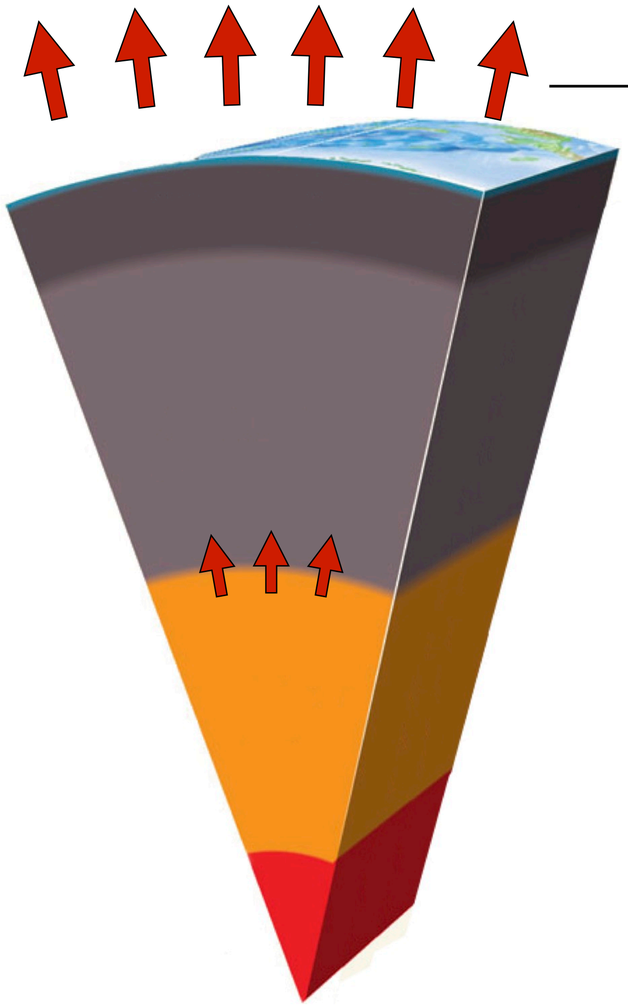




Fuel gauge for the hybrid Earth's engine



Basic energy balance



Surface heat flow — *Measured*

=

Cooling of the interior — ***??***

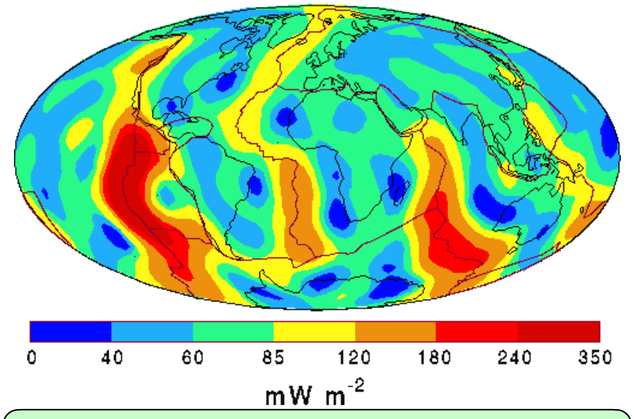
+

Heat sources — ***??***

Radioactivity

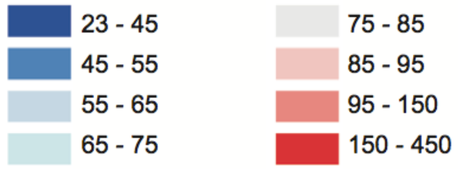
Earth's surface heat flow measurements

...supplemented with oceanic lithosphere cooling models and extrapolated in low-coverage regions:

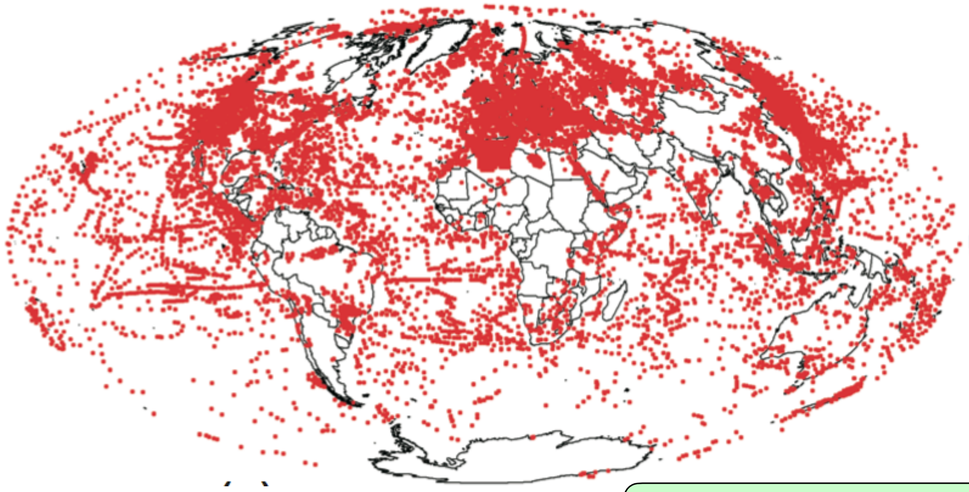


Pollack et al 1993 doi:10.1029/93RG01249

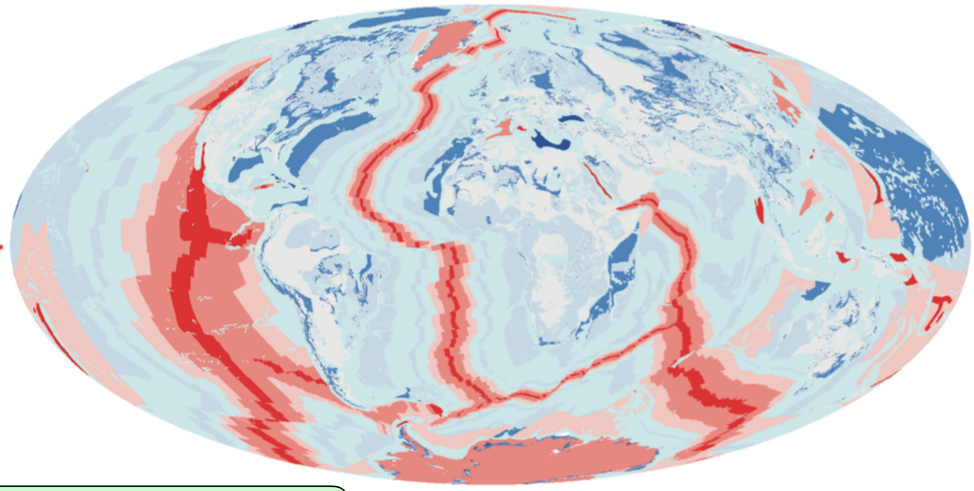
The Earth outputs 46±3 TW



measurement sites (~40000)



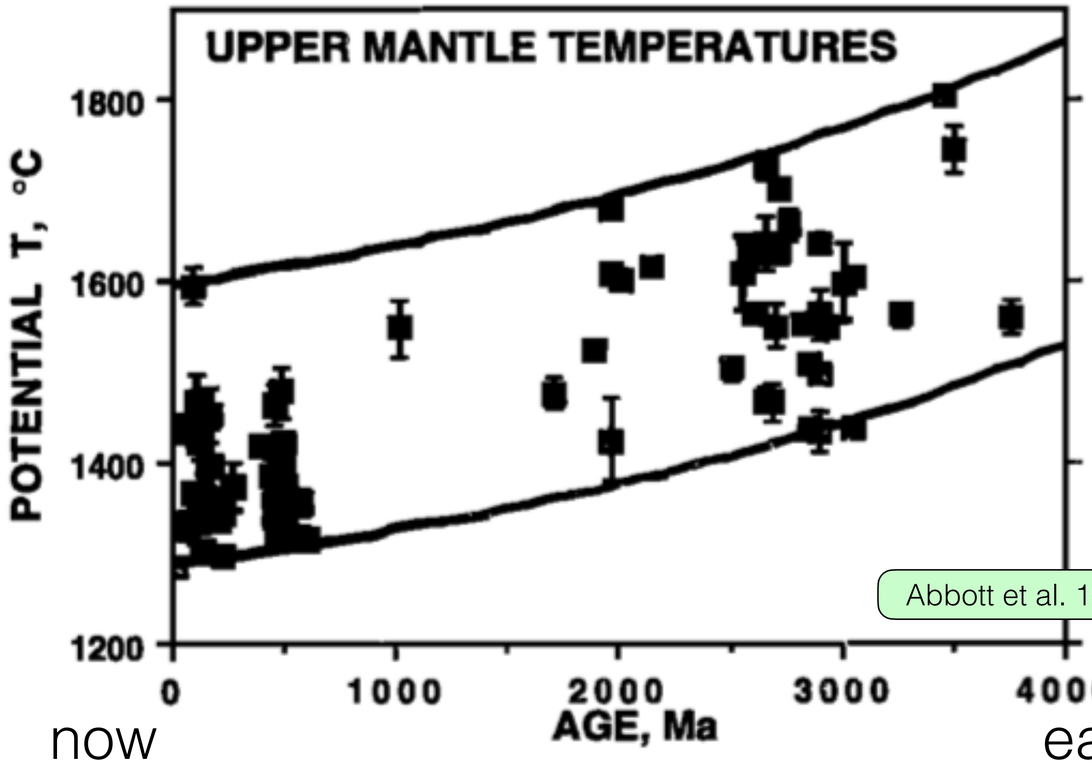
heat flux



Davies & Davies 2010 doi:10.5194/se-1-5-2010

Cooling of the interior (?)

Inference of melting temperature of upper mantle rocks



Cooling rate
50±25 K/Gy

Abbott et al. 1994 doi:10.1029/94JB00112

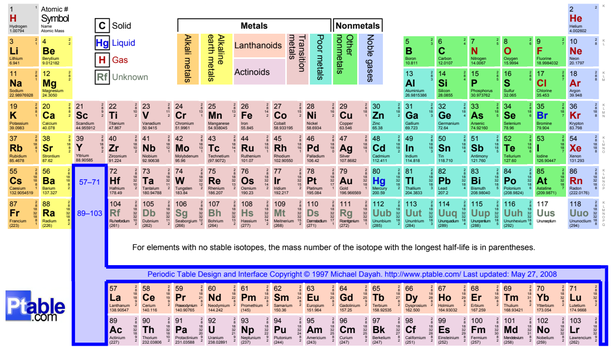
now

early Earth

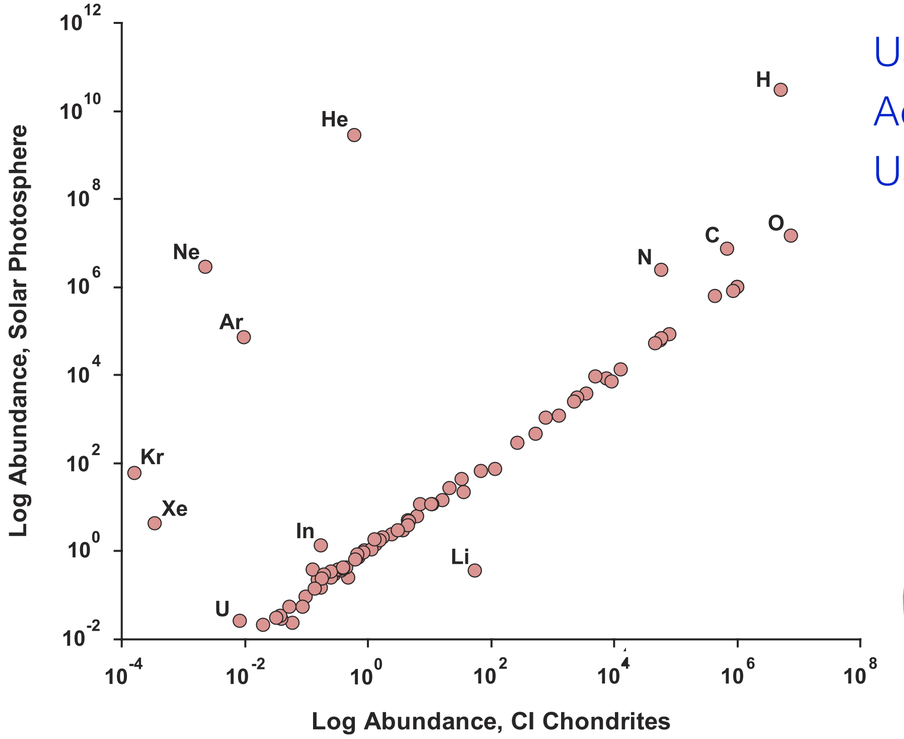
Large uncertainty on cooling rate
No information on deep Earth temperature evolution

Radiogenic heat sources (?)

- How much **U, Th, K** in the Earth ?
- … What is the Earth made of ?



Building Earth's compositional model

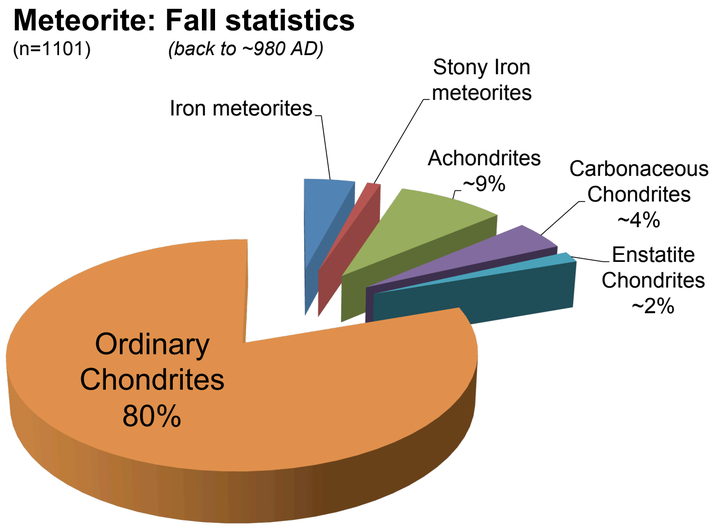


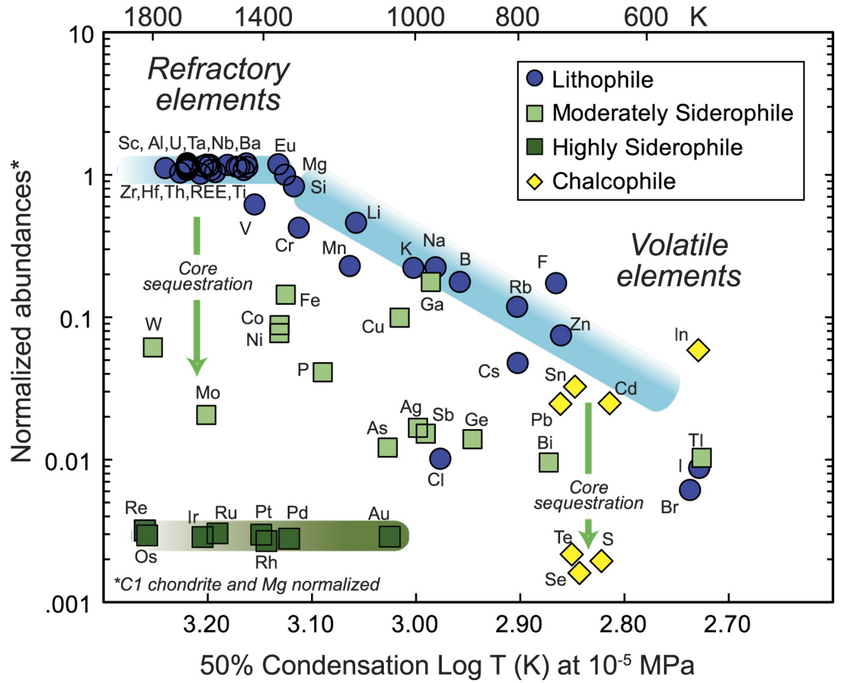
from Engel & McDonough 2016 (in: Geo-neutrinos)

Use meteorites to constrain ratios of some elements

Account for core formation

Use Earth rocks to fix absolute abundances





Radiogenic heat sources (?)

- How much **U, Th, K** in the Earth ?
- … What is the Earth made of ?

Depends on who you ask

Earth's compositional models

- **O, Fe, Si, Mg** account for **~90%** of Earth's mass
- **+ Al, Ca, Ni, S** … **>98%** of Earth's mass
- Negligible K, Th, U in the metallic core
- 10–20–30 ppb of U in **Silicate Earth**
- Th/U ratio of ~4
- K/U ratio of 7000–15000
- **10–20–30 TW** of radiogenic heating

Bulk Silicate Earth (BSE) models:

Low-H
~10 TW

Enstatite chondrite models
Collisional erosion models

Middle-H
~20 TW

Chondritic + petrological constraints

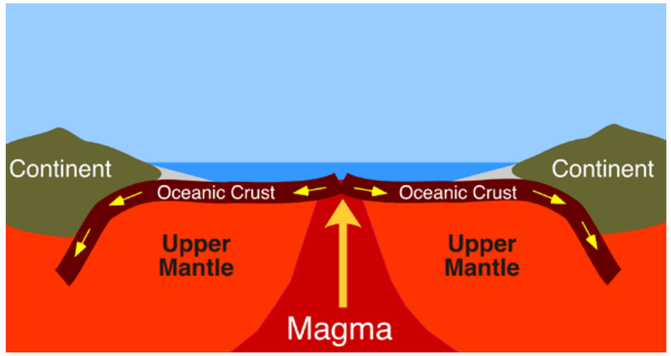
High-H
~30 TW

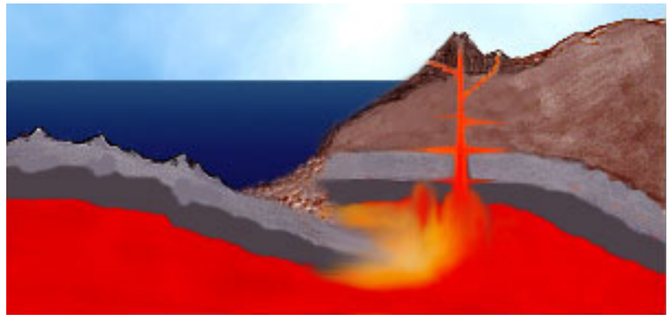
Classical parameterized convection models

A factor of 3 uncertainty in the amount of U, Th, K in the Earth…

Forming Earth's crust

"Incompatible" elements U, Th, K concentrate in the crust





Reference models for crustal radiogenic heat production

Wipperfurth et al 2020 doi:10.1029/2019JB018433

Continental Crust
7.1 (+2.1/–1.6) TW

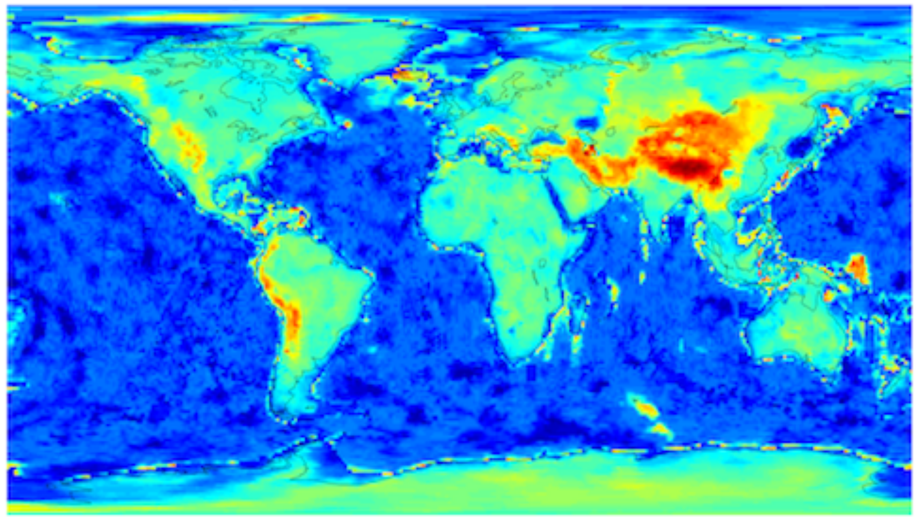
thicker (~40 km)
more enriched

Huang et al 2013 doi:10.1002/ggge.20129

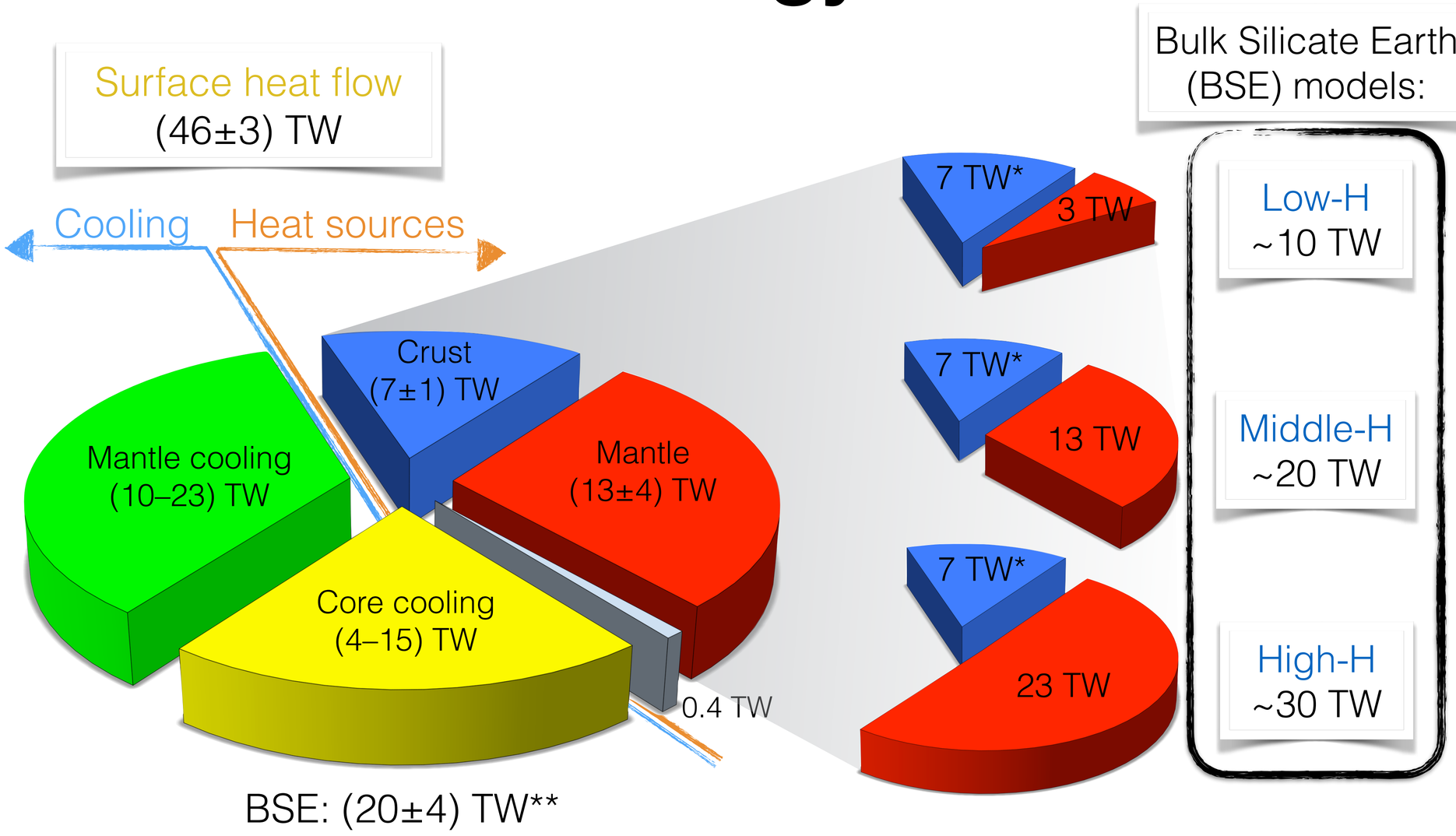
Oceanic Crust
0.22 ± 0.03 TW

thinner (~7 km)
less enriched

Radiogenic heat production in the crust



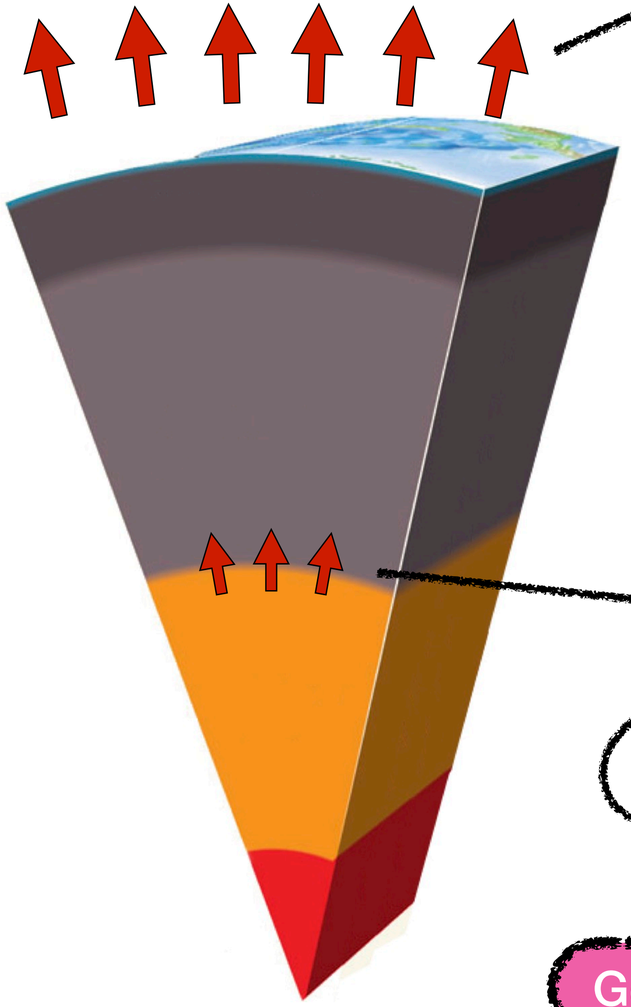
Earth's energy balance



Silicate Earth … models vary by a factor of 3
Mantle … models vary by a factor of 20

*Wipperfurth et al. (2020)
**McDonough & Sun (1995)

(Less) Basic energy balance



Surface heat flow

Measured

=

Crustal heat production

Model

+

Cooling of the mantle

??

Mantle heat sources

??

+

CMB heat flow

??

High of low??
Thermal conductivity in the core??

Cooling of the core + Inner core growth

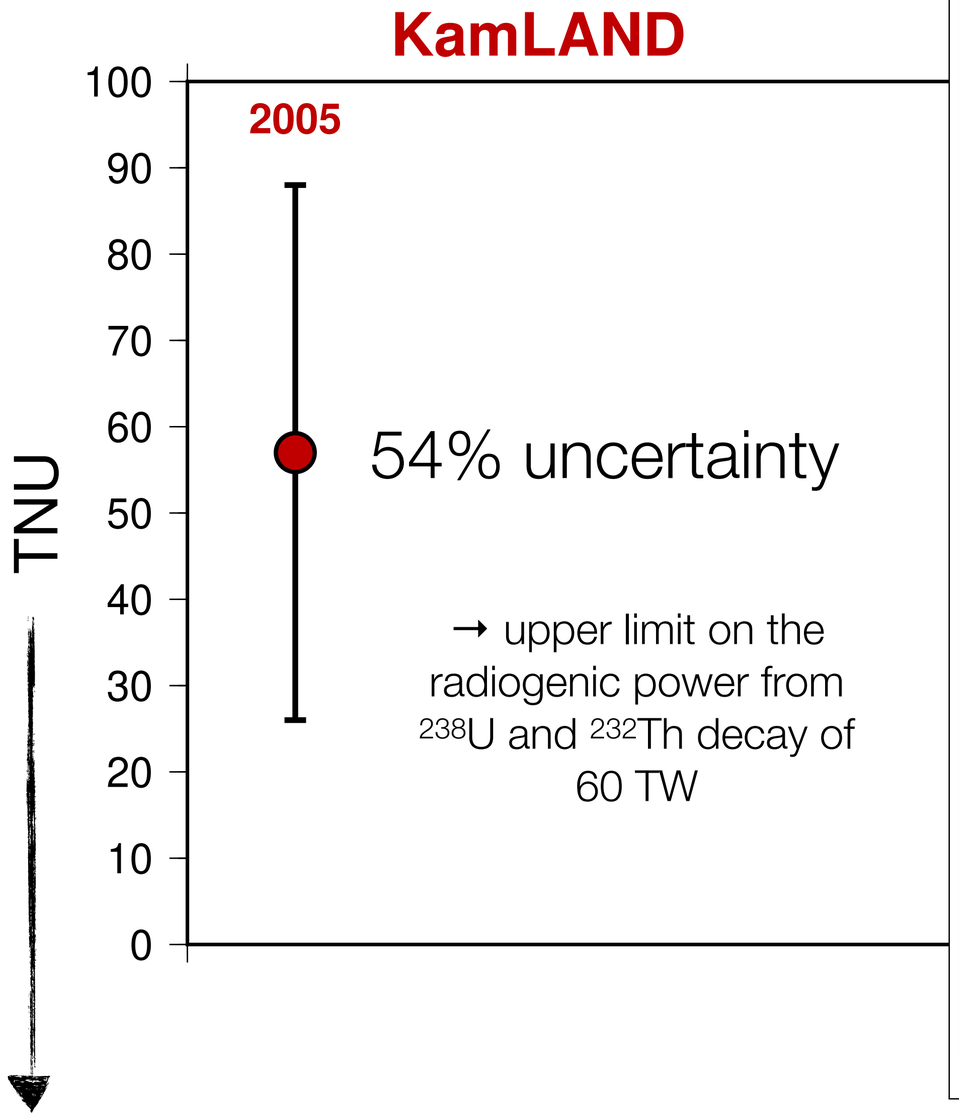
Age of inner core??

Geoneutrinos

Measured

Radioactivity

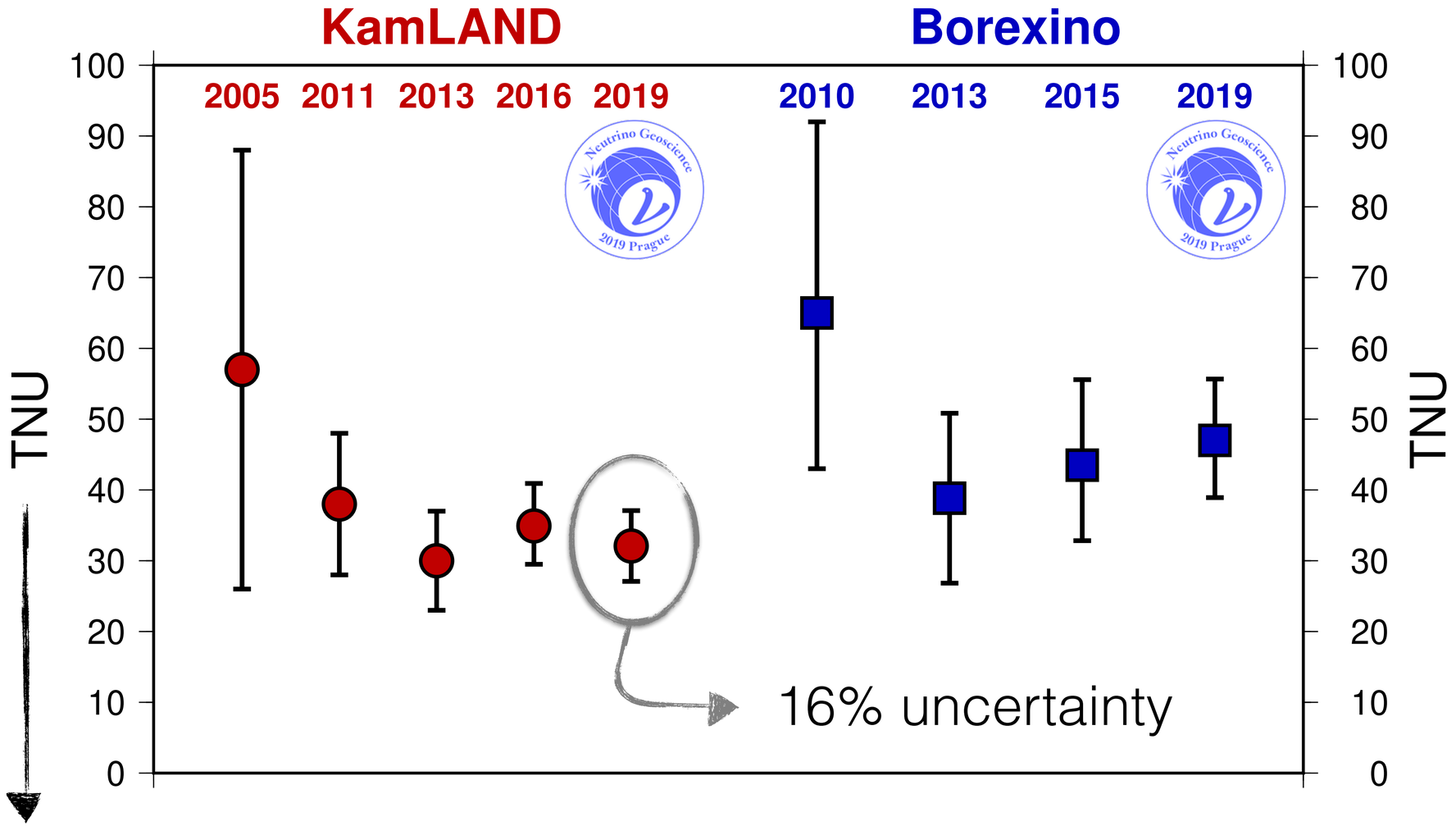
First geoneutrino measurement





1 TNU ("Terrestrial Neutrino Unit") = 1 event over a year-long IBD exposure of 10^{32} protons

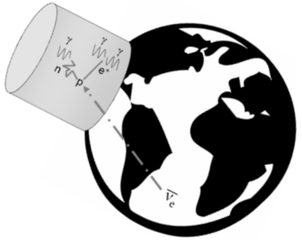
Current geoneutrino measurements



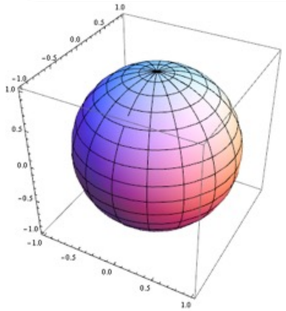
1 TNU ("Terrestrial Neutrino Unit") = 1 event over a year-long IBD exposure of 10^{32} protons

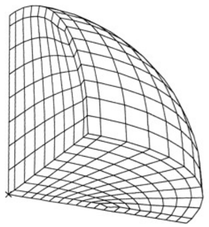
Predicting geoneutrino flux

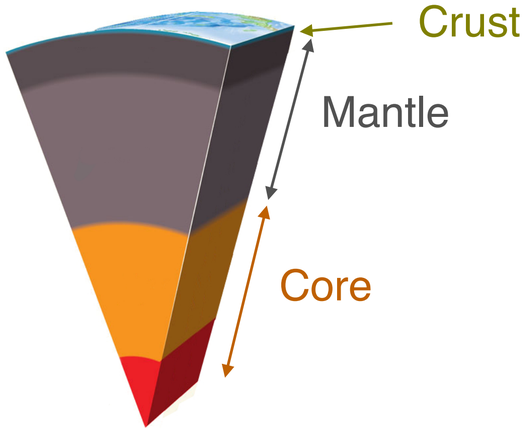
Antineutrino flux spectrum $d\Phi/dE_\nu$ at position **r** from a given radionuclide distributed with abundance A in the Earth



$$\frac{\mathrm{d}\phi(\boldsymbol{r}, E_\nu)}{\mathrm{d}E_\nu} = D\frac{\mathrm{d}n(E_\nu)}{\mathrm{d}E_\nu}\iiint \frac{A(\boldsymbol{r}')\rho(\boldsymbol{r}')P_{ee}(E_\nu, |\boldsymbol{r}-\boldsymbol{r}'|)}{4\pi|\boldsymbol{r}-\boldsymbol{r}'|^2}\mathrm{d}^3\boldsymbol{r}'$$







Inputs from geoscience:

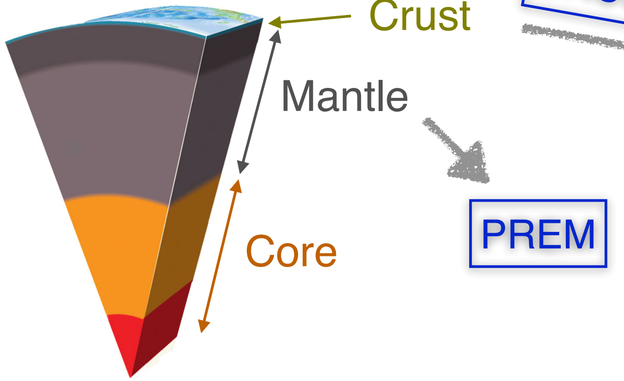
- chemical abundances A:
- density ρ

Inputs from nuclear/particle physics:

- decay rate D
- antineutrino intensity spectrum dn/dE_ν,
- antineutrino survival probability P_{ee}

Geoneutrino emission model

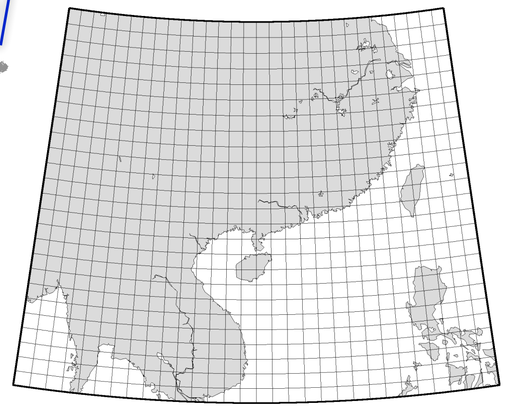
- Model of crustal geometry and material density from a global crustal model (e.g., **CRUST1.0** , **LITHO1.0**)
- Material density in the mantle from **PREM** model (*Dziewonski & Anderson 1981*)
- Assume negligible Th, U in the core
- Total amount of Th, U in **Silicate Earth** from geochemical estimates (e.g., *Arevalo et al. 2009*, **20±4 TW** rad. power)



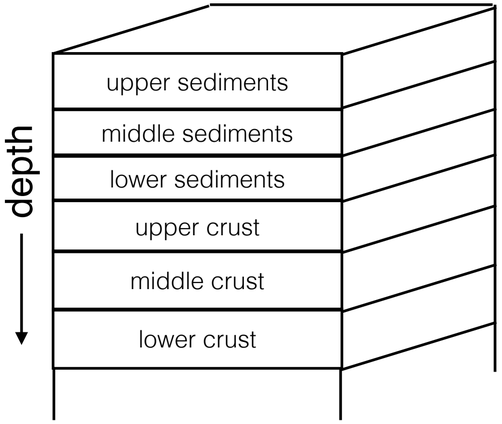
CRUST1.0

PREM

1° lat × 1° lon crustal tiles

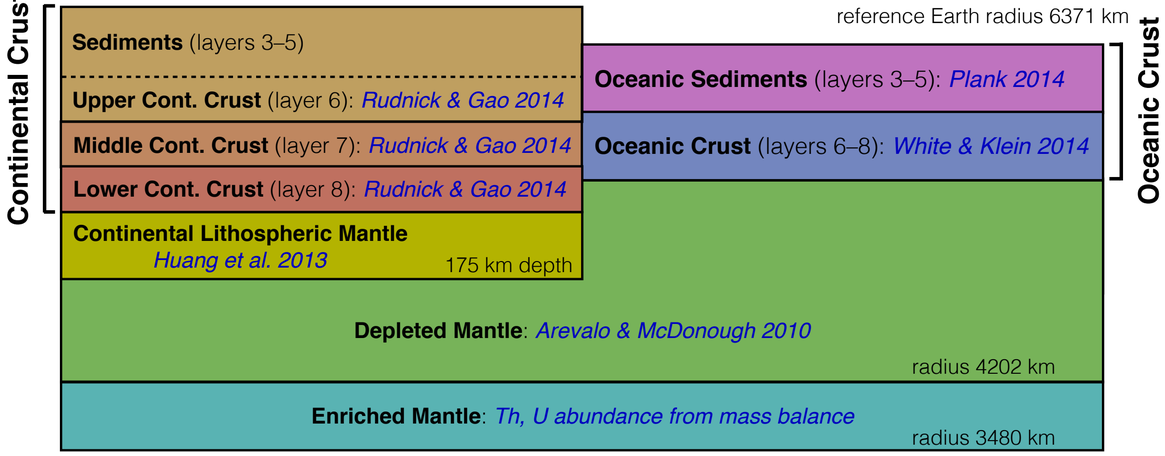


Vertical structure of a crustal tile



Continental

Oceanic

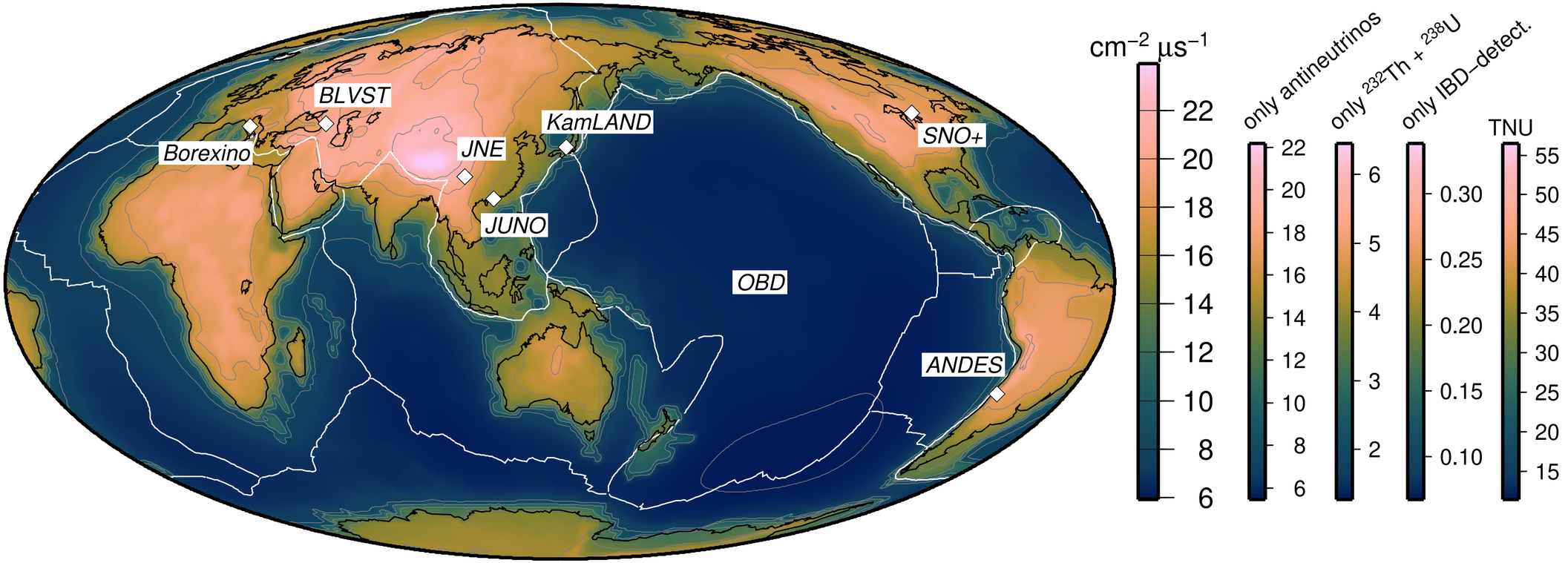


Mass fractions of Th and U

	Th	U
Upper CC + sediments	$(10.5 \pm 10\%) \times 10^{-6}$	$(2.7 \pm 21\%) \times 10^{-6}$
Middle CC	$(6.5 \pm 8\%) \times 10^{-6}$	$(1.3 \pm 31\%) \times 10^{-6}$
Lower CC	$(1.2 \pm 30\%) \times 10^{-6}$	$(0.2 \pm 30\%) \times 10^{-6}$
OC sediments	$(8.10 \pm 7\%) \times 10^{-6}$	$(1.73 \pm 5\%) \times 10^{-6}$
OC crust	$(0.21 \pm 30\%) \times 10^{-6}$	$(0.07 \pm 30\%) \times 10^{-6}$
CLM	$150^{+277}_{-97} \times 10^{-9}$	$33^{+49}_{-20} \times 10^{-9}$
Depleted Mantle	$(21.9 \pm 20\%) \times 10^{-9}$	$(8.0 \pm 20\%) \times 10^{-9}$
Enriched Mantle*	$147^{+74}_{-57} \times 10^{-9}$	$30^{+24}_{-18} \times 10^{-9}$
Bulk Silicate Earth	$(80 \pm 15\%) \times 10^{-9}$	$(20 \pm 20\%) \times 10^{-9}$

Geoneutrino flux prediction

at Earth's surface



Šrámek 2020 doi:10.1016/B978-0-08-102908-4.00161-2

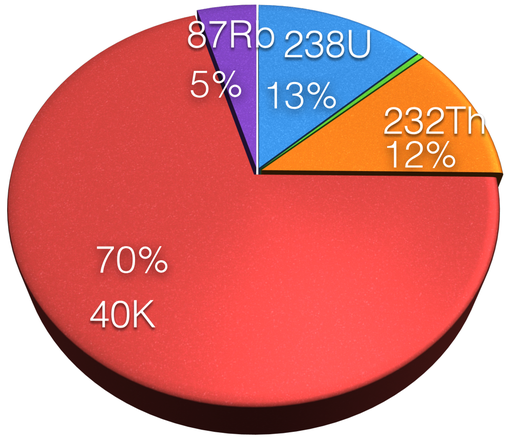
It looks like a crustal thickness map.

Radiogenic power and antineutrino luminosity of the Earth

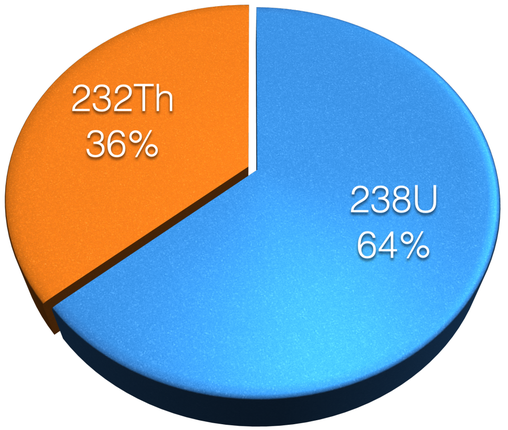
Earth model:
- 20 ppb U
- Th/U = 4
- K/U = 14000
- Rb/U = 30

in BSE

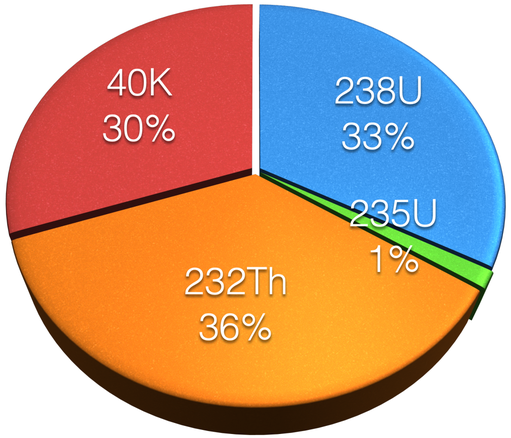
BSE antineutrino **luminosity** = 4.3e25 per second



IBD-detectable antineutrino **luminosity** = 6.2e23 per sec



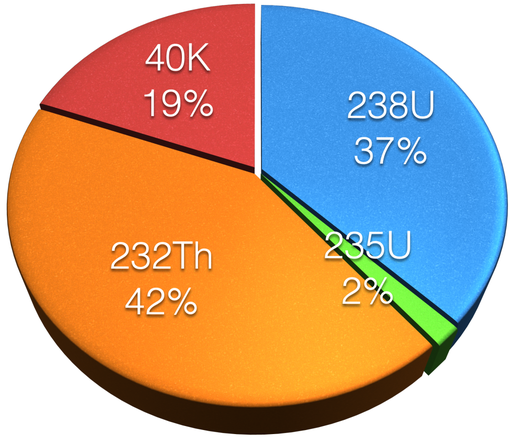
BSE decay **power** = 25.2 TW



100%
total energy released in decays

=

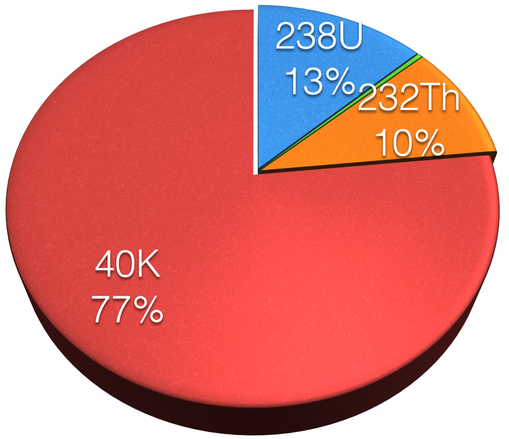
BSE radiogenic heat = 20.4 TW



81%
heats the Earth

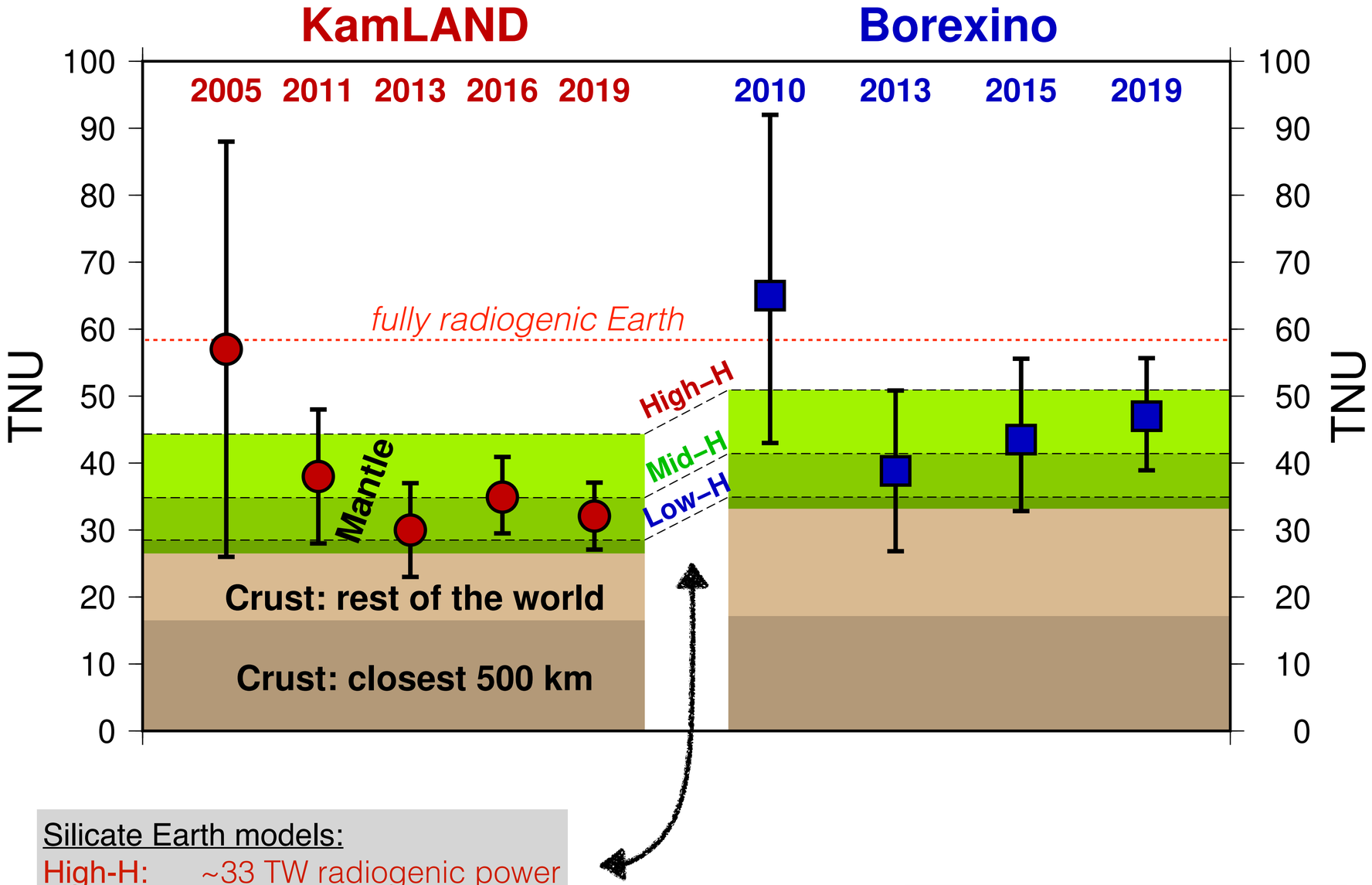
+

BSE neutrino **power** = 4.8 TW



19%
lost to space

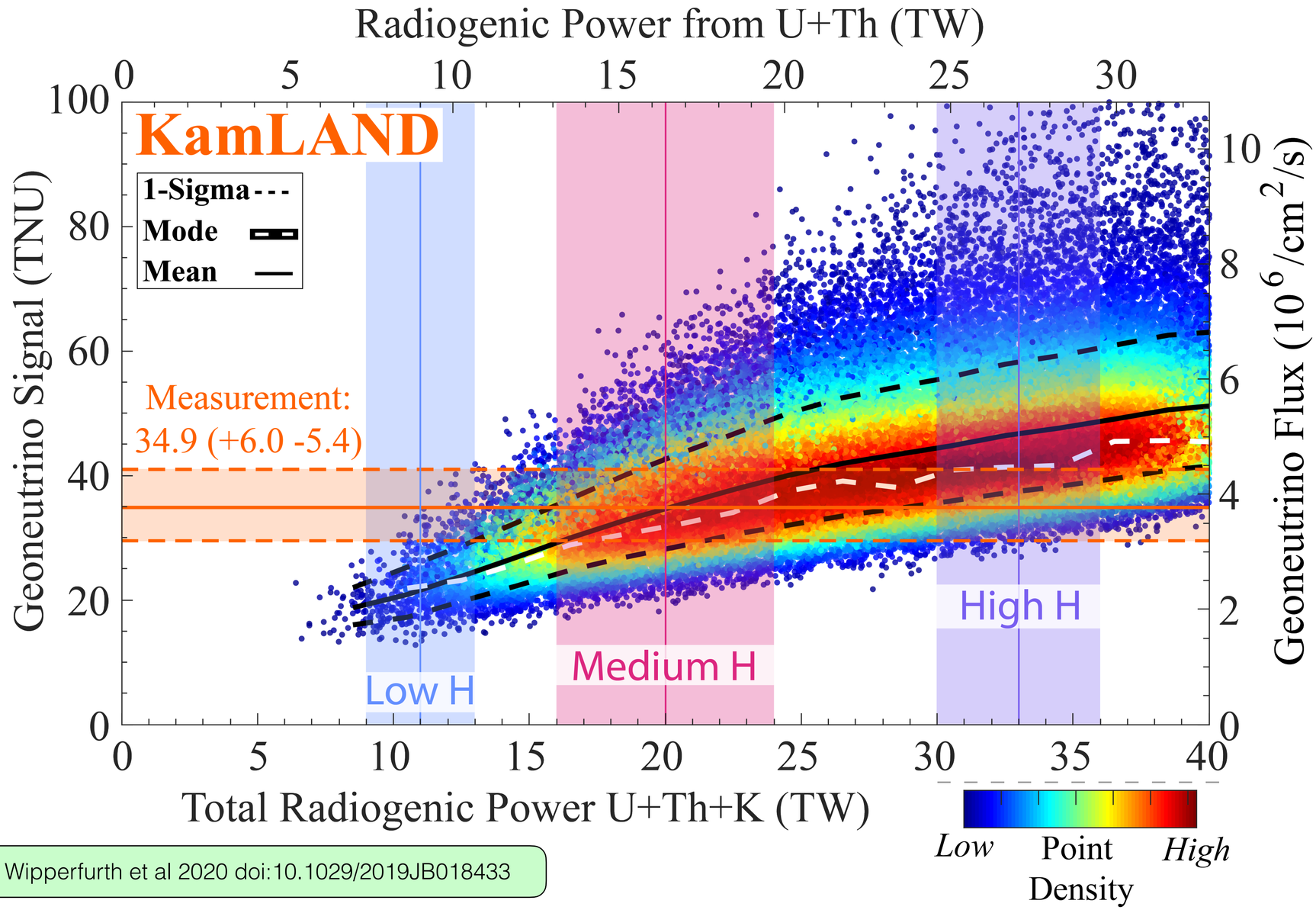
Geoneutrinos measurements vs. predictions



Silicate Earth models:
High-H: ~33 TW radiogenic power
Medium-H: ~20 TW
Low-H: ~11 TW

Geoneutrino prediction from
Šrámek et al. 2016 doi:10.1038/srep33034

Interpreting geoneutrino signal in terms of radiogenic power



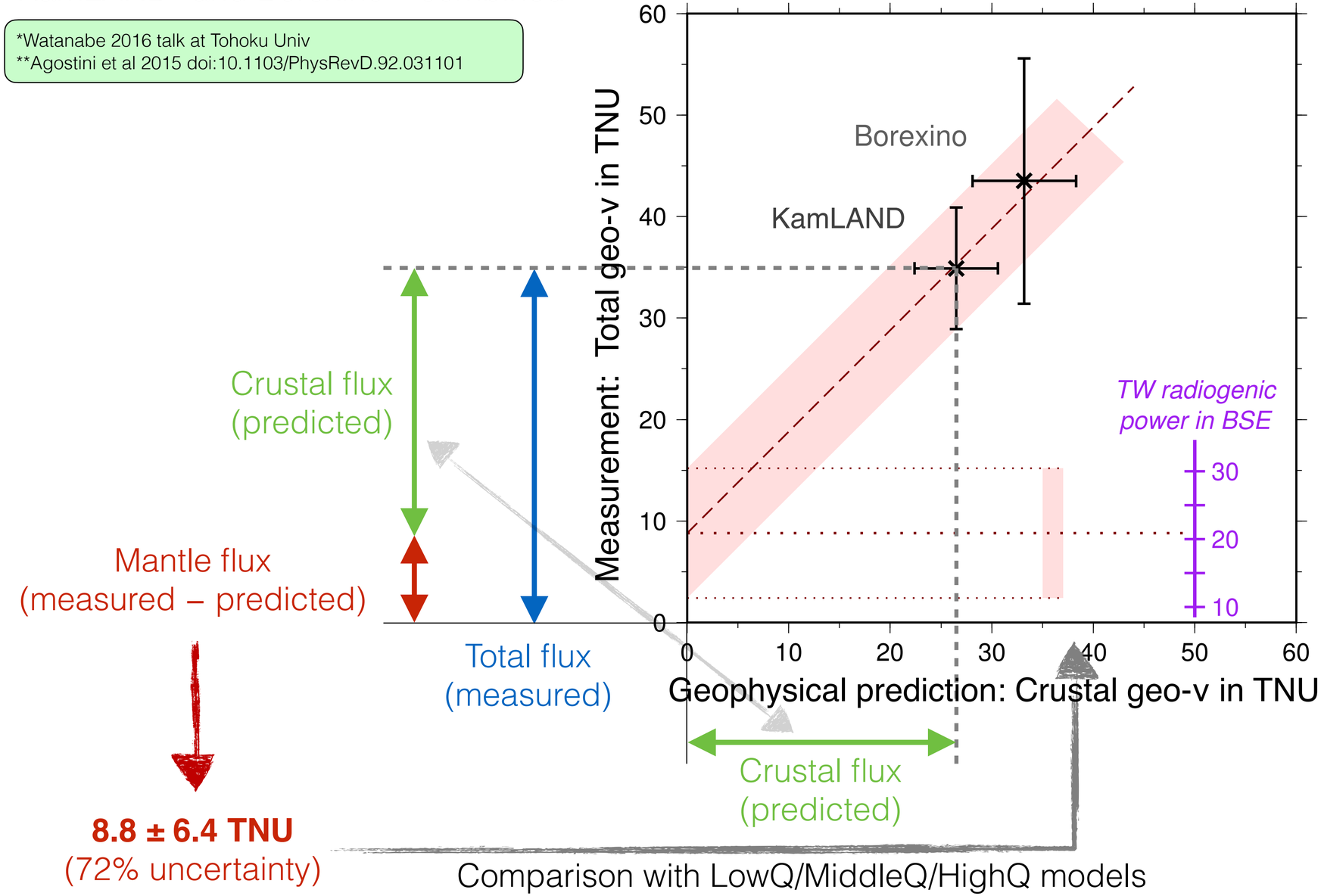
Wipperfurth et al 2020 doi:10.1029/2019JB018433

“Measuring” the mantle (as of 2016)

KamLAND* and Borexino** combined

*Watanabe 2016 talk at Tohoku Univ
**Agostini et al 2015 doi:10.1103/PhysRevD.92.031101

Šrámek et al 2016 doi:10.1038/srep33034



“The 2019 Prague Geoneutrino Schism”



Ilustrační foto: “X-Men: SCHISM” (http://www.comicartcommunity.com/gallery/details.php?image_id=57038)

“The 2019 Prague Geoneutrino Schism”

Watanabe 2019 at NGS Prague

KamLAND

Measured signal 32.1 ± 5.0 TNU

After subtracting crustal prediction:

Mantle signal **$6.0^{+5.6}_{-5.7}$ TNU**

Corresponds to **~15 TW** (±?) in the Earth

or **~8 TW** in the mantle

giving **mantle Urey ratio of ~0.21**

Agostini et al 2020 doi:10.1103/PhysRevD.101.012009

Borexino

Measured signal $47.0^{+8.6}_{-8.1}$ TNU

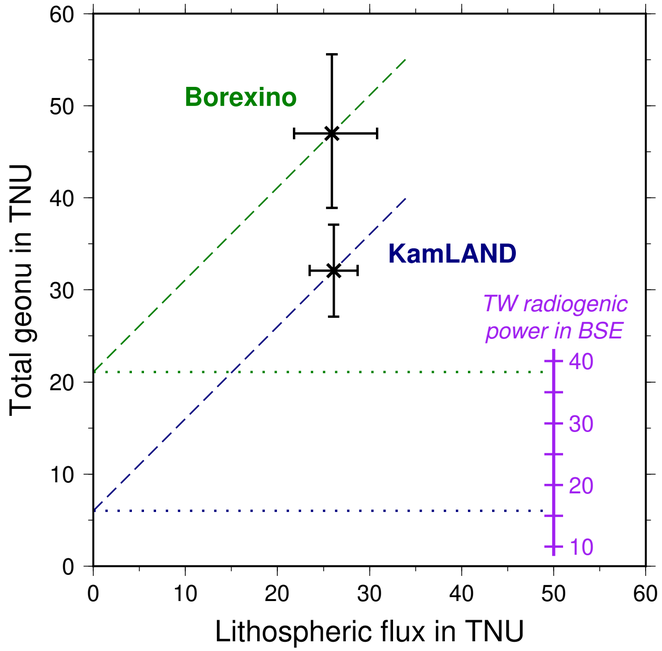
After subtracting crustal prediction:

Mantle signal **$21.0^{+9.6}_{-9.0}$ TNU**

Corresponds to **$38.2^{+13.6}_{-12.7}$ TW** in the Earth

or **$30.1^{+13.5}_{-12.7}$ TW** in the mantle

giving **mantle Urey ratio of $0.78^{+0.41}_{-0.28}$**



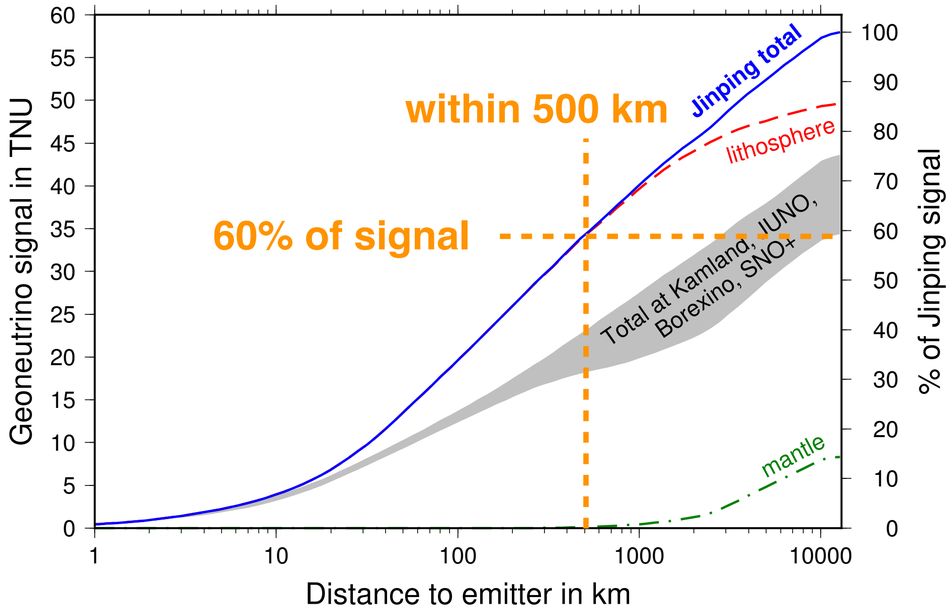
Factor of 3.5 difference in mantle radiogenic power!!!

Possible explanations:

1. There is a problem with the geoneutrino measurments (nope)
2. Look at uncertainties and it is all consistent (hmm…)
3. There is a very different mantle below Japan and below Italy (unlikely)
4. There is something funky with at least one of the crustal models (bingo)

Ongoing effort to understand the discrepancy.

Significance of nearby crust



$$\frac{\mathrm{d}\phi(\boldsymbol{r}, E_\nu)}{\mathrm{d}E_\nu} = D\frac{\mathrm{d}n(E_\nu)}{\mathrm{d}E_\nu}\iiint \frac{A(\boldsymbol{r}')\rho(\boldsymbol{r}')P_{ee}(E_\nu, |\boldsymbol{r}-\boldsymbol{r}'|)}{4\pi|\boldsymbol{r}-\boldsymbol{r}'|^2}\mathrm{d}^3\boldsymbol{r}'$$

~half of geoneutrino signal originates within ~500 km around the detector

Need for crustal model accurate both at the global scale and at the local scale around detectors.

seismic models of the crust V_P, V_S ⟷ seismic speed — rock type relationships → SiO_2 ⟷ rock type — chemistry relationships → Th, U

Wipperfurth et al 2020 doi:10.1029/2019JB018433
Laura Sammon (Univ Maryland) ongoing PhD work

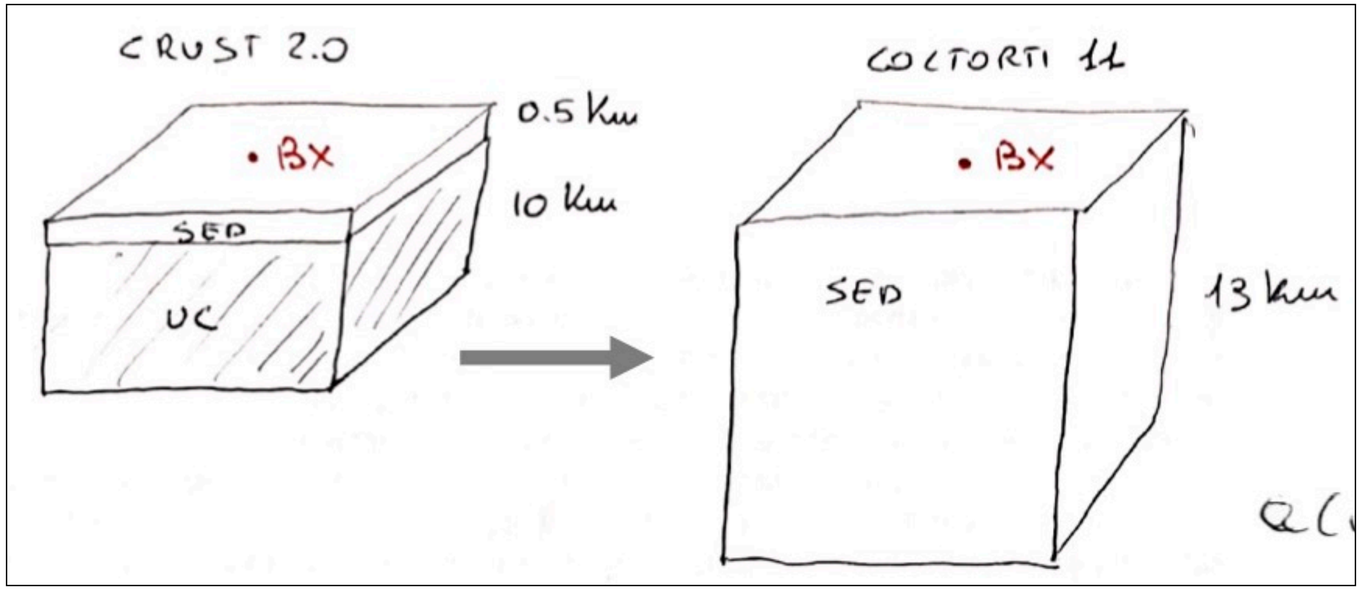
+ local geology
geochemical analyses of available rocks
gravity, heat flux, …

Why the difference between KL and BX?

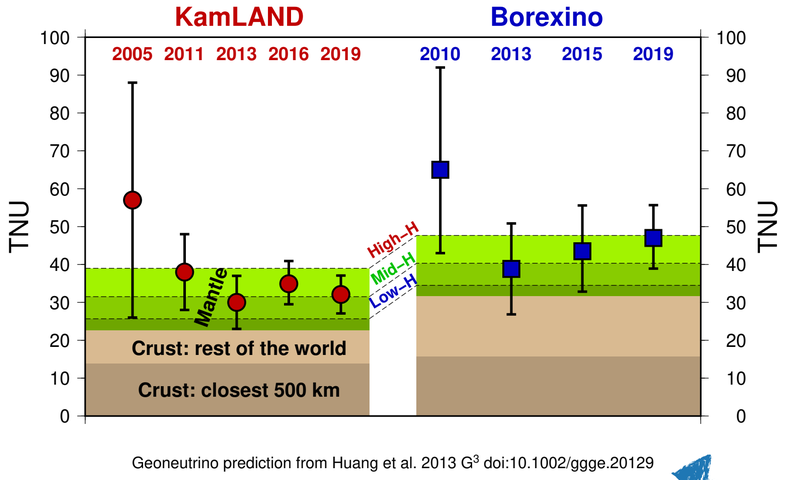
KamLAND

Borexino

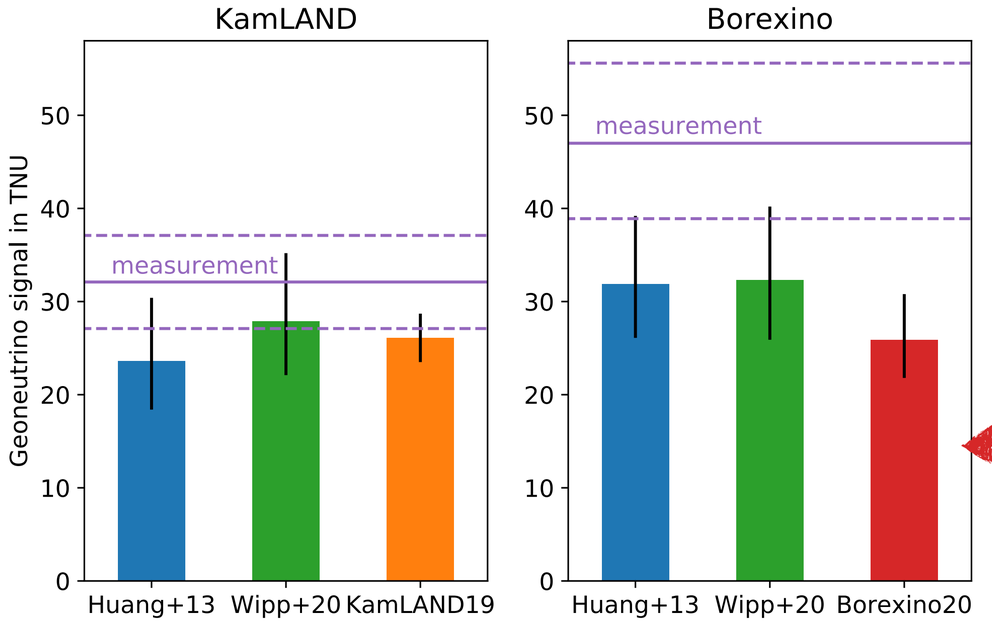
- No sudden shift in the measured value of geoneutrino flux.
- Differences in global crustal model predictions are minimal.
- **The Borexino team has radically changed their local crustal model.**

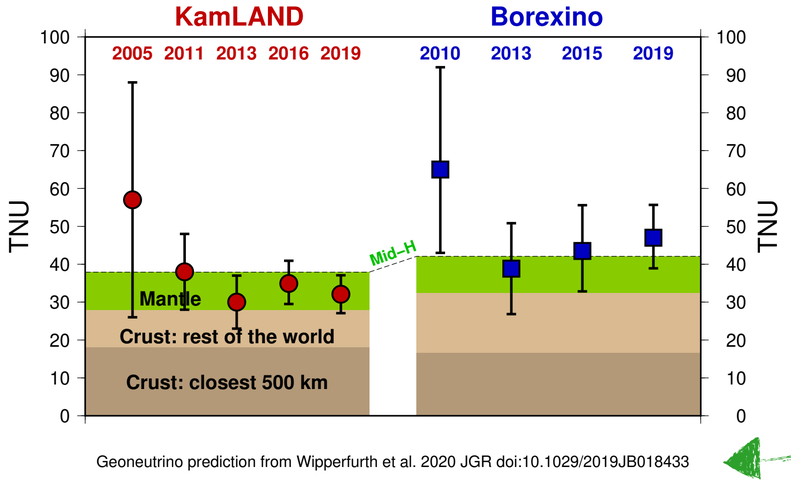


13 km thick layer of “limestone” sediments surrounding the detector

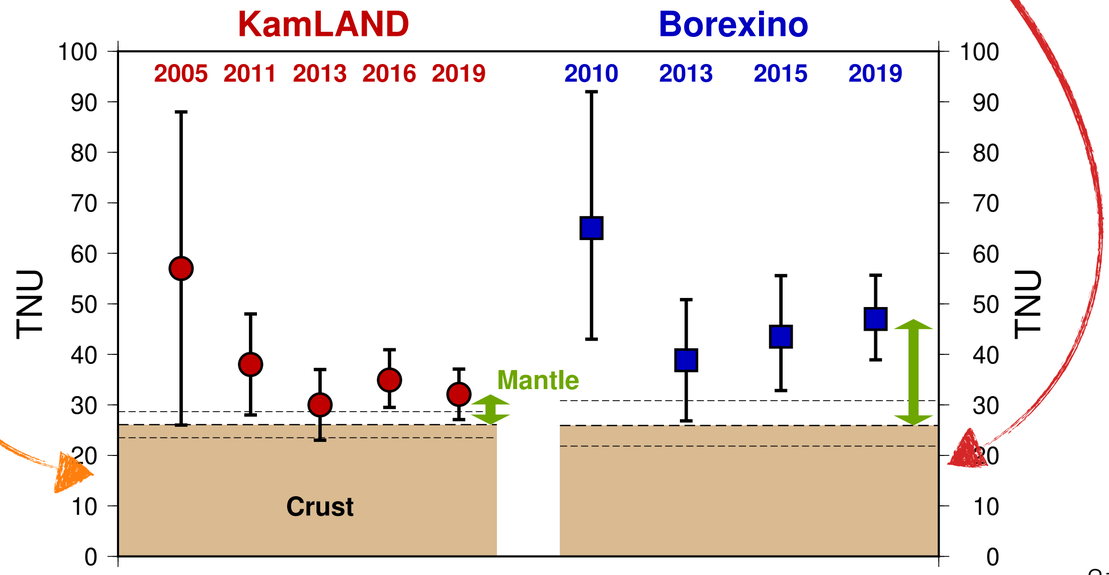


Geoneutrino prediction from Huang et al. 2013 G^3 doi:10.1002/ggge.20129

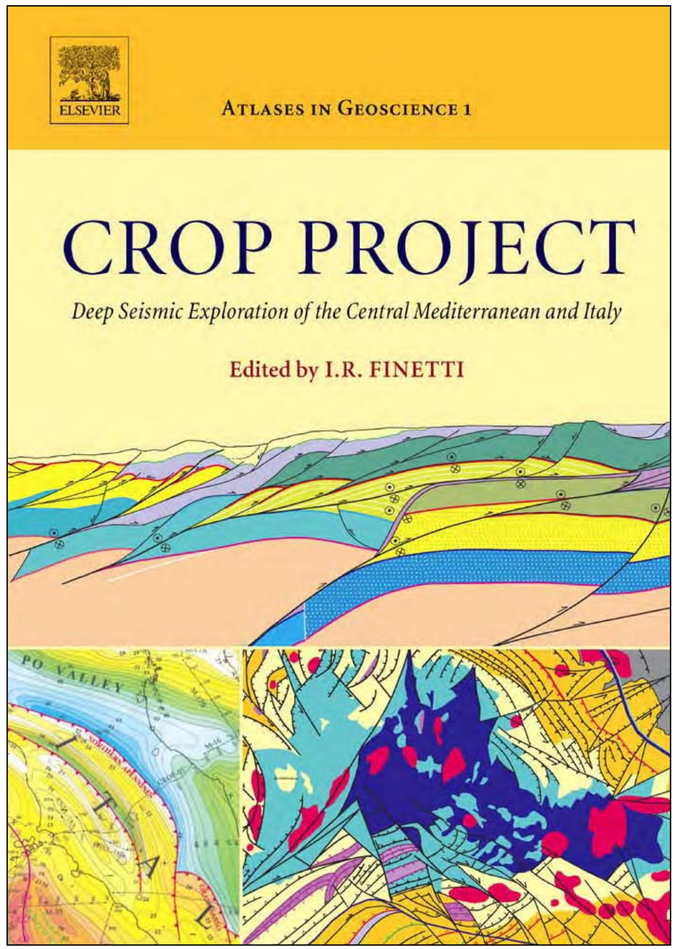




Geoneutrino prediction from Wipperfurth et al. 2020 JGR doi:10.1029/2019JB018433



Borexino local crustal model



ELSEVIER

Available online at www.sciencedirect.com
ScienceDirect
Geochimica et Cosmochimica Acta 75 (2011) 2271–2294

Geochimica et Cosmochimica Acta
www.elsevier.com/locate/gca

U and Th content in the Central Apennines continental crust: A contribution to the determination of the geo-neutrinos flux at LNGS

M. Coltorti [a,*], R. Boraso [a], F. Mantovani [b,e], M. Morsilli [a], G. Fiorentini [b,e], A. Riva [a], G. Rusciadelli [c], R. Tassinari [a], C. Tomei [d], G. Di Carlo [d], V. Chubakov [b,e]

[a] *Dipartimento di Scienze della Terra, Università di Ferrara, Italy*
[b] *Dipartimento di Fisica, Università di Ferrara, Italy*
[c] *Dipartimento di Scienze della Terra, Università di Chieti, Italy*
[d] *INFN, Laboratorio Nazionale Gran Sasso, Italy*
[e] *INFN, Sezione di Ferrara, Italy*

Received 16 June 2010; accepted in revised form 18 January 2011; available online 23 January 2011

Abstract

The regional contribution to the geo-neutrino signal at Gran Sasso National Laboratory (LNGS) was determined based on a detailed geological, geochemical and geophysical study of the region. U and Th abundances of more than 50 samples representative of the main lithotypes belonging to the Mesozoic and Cenozoic sedimentary cover were analyzed. Sedimentary rocks were grouped into four main "reservoirs" based on similar depositional settings and mineralogy. The initial assumption that similar chemico-physical depositional conditions would lead to comparable U and Th contents, was then confirmed by chemical analyses. Basement rocks do not outcrop in the area. Thus U and Th in the upper and lower crust of Valsugana and Ivrea–Verbano areas were analyzed. Irrespective of magmatic or metamorphic origin lithotypes were subdivided into a mafic and an acid reservoir, with comparable U and Th abundances.

Based on geological and geophysical properties, relative abundances of the various reservoirs were calculated and used to obtain the weighted U and Th abundances for each of the three geological layers (sedimentary cover, upper and lower crust). Using the available seismic profile as well as the stratigraphic records from a number of exploration wells, a 3D modeling was developed over an area of 2° × 2° down to the Moho depth, for a total volume of about 1.2×10^6 km^3. This model allowed us to determine the volume of the various geological layers and eventually integrate the Th and U contents of the whole crust beneath LNGS.

On this base the local contribution to the geo-neutrino flux (S) was calculated and added to the contribution given by the rest of the world, yielding a refined reference model prediction for the geo-neutrino signal in the Borexino detector at LNGS: $S(U) = (28.7 \pm 3.9)$ TNU and $S(Th) = (7.5 \pm 1.0)$ TNU. An excess over the total flux of about 4 TNU was previously obtained by Mantovani et al. (2004) who calculated, based on general worldwide assumptions, a signal of 40.5 TNU. The considerable thickness of the sedimentary rocks, almost predominantly represented by U- and Th-poor carbonatic rocks in the area near LNGS, is responsible for this difference. Thus the need for detailed integrated geological study is underlined by this work, if the usefulness of the geo-neutrino flux for characterizing the global U and Th distribution within the Earth's crust, mantle and core is to be realized.
© 2011 Elsevier Ltd. All rights reserved.

* Corresponding author. Address: Dipartimento di Scienze della Terra, Via Saragat 1, 44100 Ferrara, Italy. Tel.: +39 0532 974721; fax: +39 0532 974767.
E-mail address: clt@unife.it (M. Coltorti).

0016-7037/$ - see front matter © 2011 Elsevier Ltd. All rights reserved.
doi:10.1016/j.gca.2011.01.024

1. INTRODUCTION

Geo-neutrinos—the antineutrinos from the decay of U, Th and ^{40}K in the Earth—can provide information on the

PHYSICAL REVIEW D **101,** 012009 (2020)

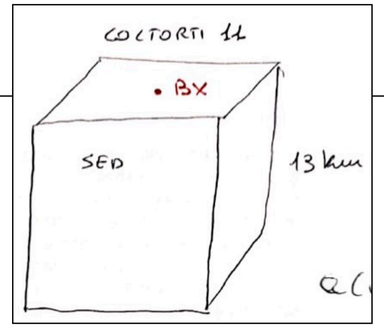
Editors' Suggestion | Featured in Physics

Comprehensive geoneutrino analysis with Borexino

M. Agostini,[16] K. Altenmüller,[16] S. Appel,[16] V. Atroshchenko,[6] Z. Bagdasarian,[22] D. Basilico,[9] G. Bellini,[9] J. Benziger,[13] D. Bick,[26] G. Bonfini,[8] D. Bravo,[9,c] B. Caccianiga,[9] F. Calaprice,[12] A. Caminata,[3] L. Cappelli,[8] P. Cavalcante,[15,e] F. Cavanna,[3] A. Chepurnov,[17] K. Choi,[21] D. D'Angelo,[9] S. Davini,[3] A. Derbin,[11] A. Di Giacinto,[8] V. Di Marcello,[8] X. F. Ding,[18,8,12] A. Di Ludovico,[12] L. Di Noto,[3] I. Drachnev,[11] G. Fiorentini,[28,29] A. Formozov,[2,9,17] D. Franco,[1] F. Gabriele,[8] C. Galbiati,[12] M. Gschwender,[24] C. Ghiano,[8] M. Giammarchi,[9] A. Goretti,[12,c] M. Gromov,[17,2] D. Guffanti,[18,8,f] C. Hagner,[26] E. Hungerford,[25] Aldo Ianni,[8] Andrea Ianni,[12] A. Jany,[4] D. Jeschke,[16] S. Kumaran,[22,23] V. Kobychev,[5] G. Korga,[25,g] T. Lachenmaier,[24] T. Lasserre,[27] M. Laubenstein,[8] E. Litvinovich,[6,7] P. Lombardi,[9] I. Lomskaya,[11] L. Ludhova,[22,23] G. Lukyanchenko,[6] L. Lukyanchenko,[6] I. Machulin,[6,7] F. Mantovani,[28,29] G. Manuzio,[3] S. Marcocci,[18,f,g] J. Maricic,[21] J. Martyn,[20,f] E. Meroni,[9] M. Meyer,[19] L. Miramonti,[9] M. Misiaszek,[4] M. Montuschi,[28,29] V. Muratova,[11] B. Neumair,[16] M. Nieslony,[20,f] L. Oberauer,[16] A. Onillon,[27] V. Orekhov,[20,f] F. Ortica,[10] M. Pallavicini,[3] L. Papp,[16] Ö. Penek,[22,23] L. Pietrofaccia,[12] N. Pilipenko,[11] A. Pocar,[14] G. Raikov,[6] M.T. Ranalli,[8] G. Ranucci,[9] A. Razeto,[8] A. Re,[9] M. Redchuk,[22,23] B. Ricci,[28,29] A. Romani,[10] N. Rossi,[8,a] S. Rottenanger,[24] S. Schönert,[16] D. Semenov,[11] M. Skorokhvatov,[6,7] O. Smirnov,[2] A. Sotnikov,[2] V. Strati,[8,6,8] R. Tartaglia,[8] G. Testera,[3] J. Thurn,[19] E. Unzhakov,[11] A. Vishneva,[2] M. Vivier,[27] R.B. Vogelaar,[15] F. von Feilitzsch,[16] M. Wojcik,[4] M. Wurm,[20,f] O. Zaimidoroga,[2,1] S. Zavatarelli,[3] K. Zuber,[19] and G. Zuzel[4]

(Borexino Collaboration)*

[1] *AstroParticule et Cosmologie, Université Paris Diderot, CNRS/IN2P3, CEA/IRFU, Observatoire de Paris, Sorbonne Paris Cité, 75205 Paris Cedex 13, France*
[2] *Joint Institute for Nuclear Research, 141980 Dubna, Russia*
[3] *Dipartimento di Fisica, Università degli Studi e INFN, 16146 Genova, Italy*
[4] *M. Smoluchowski Institute of Physics, Jagiellonian University, 30348 Krakow, Poland*
[5] *Kiev Institute for Nuclear Research, 03680 Kiev, Ukraine*
[6] *National Research Centre Kurchatov Institute, 123182 Moscow, Russia*
[7] *National Research Nuclear University MEPhI (Moscow Engineering Physics Institute), 115409 Moscow, Russia*
[8] *INFN Laboratori Nazionali del Gran Sasso, 67010 Assergi (AQ), Italy*
[9] *Dipartimento di Fisica, Università degli Studi e INFN, 20133 Milano, Italy*
[10] *Dipartimento di Chimica, Biologia e Biotecnologie, Università degli Studi e INFN, 06123 Perugia, Italy*
[11] *St. Petersburg Nuclear Physics Institute NRC Kurchatov Institute, 188350 Gatchina, Russia*
[12] *Physics Department, Princeton University, Princeton, New Jersey 08544, USA*
[13] *Chemical Engineering Department, Princeton University, Princeton, New Jersey 08544, USA*
[14] *Amherst Center for Fundamental Interactions and Physics Department, University of Massachusetts, Amherst, Massachusetts 01003, USA*
[15] *Physics Department, Virginia Polytechnic Institute and State University, Blacksburg, Virginia 24061, USA*
[16] *Physik-Department and Excellence Cluster Universe, Technische Universität München, 85748 Garching, Germany*
[17] *Lomonosov Moscow State University Skobeltsyn Institute of Nuclear Physics, 119234 Moscow, Russia*
[18] *Gran Sasso Science Institute, 67100 L'Aquila, Italy*
[19] *Department of Physics, Technische Universität Dresden, 01062 Dresden, Germany*
[20] *Institute of Physics and Excellence Cluster PRISMA*, Johannes Gutenberg-Universität Mainz, 55099 Mainz, Germany*
[21] *Department of Physics and Astronomy, University of Hawaii, Honolulu, Hawaii 96822, USA*
[22] *Institut für Kernphysik, Forschungszentrum Jülich, 52425 Jülich, Germany*
[23] *RWTH Aachen University, 52062 Aachen, Germany*
[24] *Kepler Center for Astro and Particle Physics, Universität Tübingen, 72076 Tübingen, Germany*
[25] *Department of Physics, University of Houston, Houston, Texas 77204, USA*
[26] *Institut für Experimentalphysik, Universität Hamburg, 22761 Hamburg, Germany*
[27] *IRFU, CEA, Université Paris-Saclay, F-91191 Gif-sur-Yvette, France*



Published by the American Physical Society

Sediment thickness in EPcrust

Geophysical Journal International

Geophys. J. Int. (2011) **185,** 352–364 doi: 10.1111/j.1365-246X.2011.04940.x

EPcrust: a reference crustal model for the European Plate

Irene Molinari and Andrea Morelli

Istituto Nazionale di Geofisica e Vulcanologia, Sezione di Bologna, via Donato Creti 12, 40128 *Bologna, Italy. E-mail: irene.molinari@bo.ingv.it*

Accepted 2011 January 3. Received 2010 November 17; in original form 2010 July 29

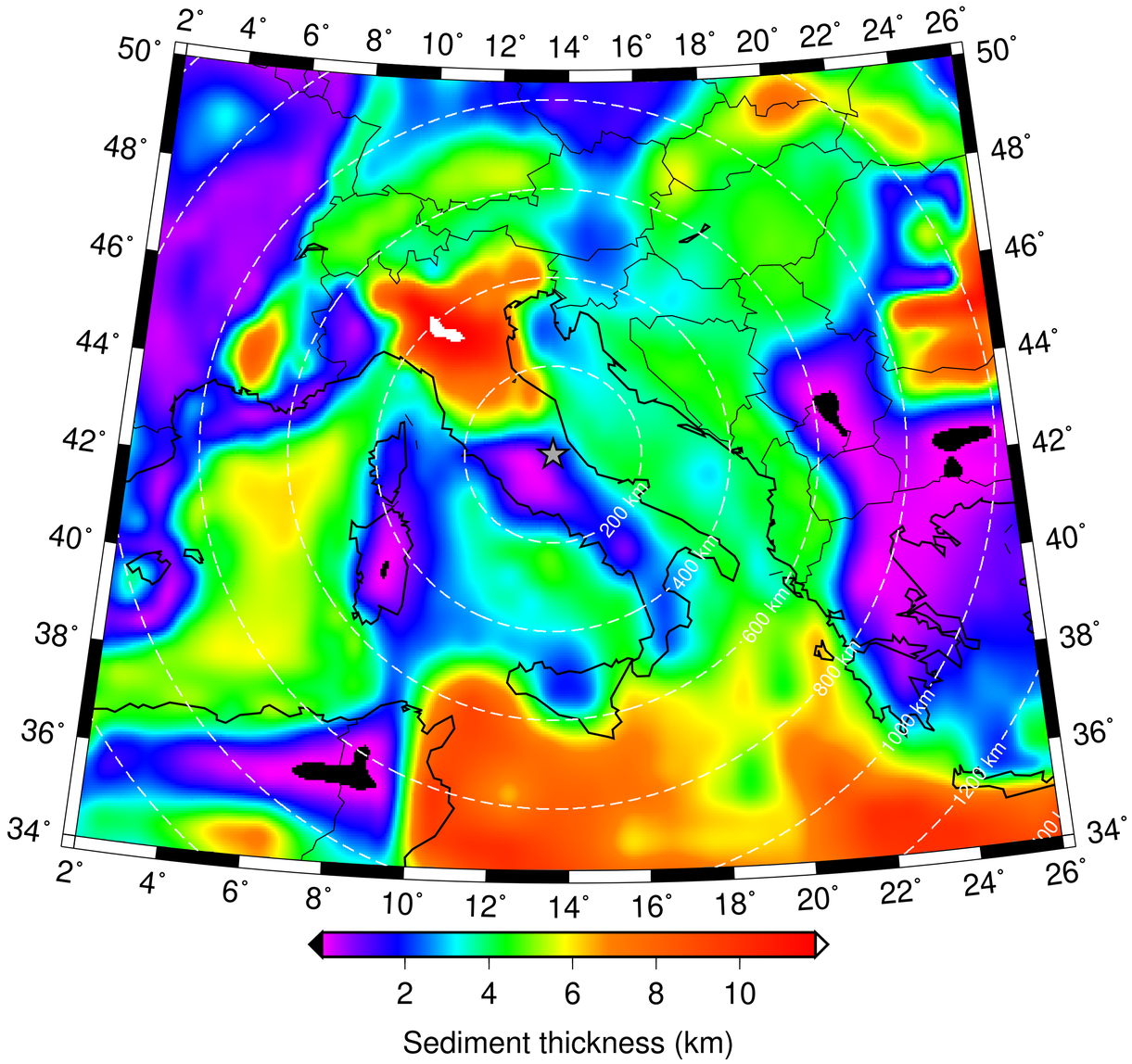
SUMMARY

We present a new crustal model for the European Plate, derived from collection and critical integration of information selected from the literature. The model covers the whole European Plate from North Africa to the North Pole (20°N–90°N) and from the Mid-Atlantic Ridge to the Urals (40°W–70°E). The chosen parametrization represents the crust in three layers (sediments, upper crust and lower crust), and describes the 3-D geometry of the interfaces and seismologically relevant parameters—isotropic *P*- and *S*-wave velocity, plus density—with a resolution of 0.5° × 0.5° on a geographical latitude–longitude grid. We selected global and local models, derived from geological assumptions, active seismic experiments, surface wave studies, noise correlation, receiver functions. Model EPcrust presents significant advantages with respect to previous models: it covers the whole European Plate; it is a complete and internally-consistent model (with all the parameters provided, also for the sedimentary layer); it is reproducible; it is easy to update in the future by adding new contributions; and it is available in a convenient digital format. EPcrust could be used to account for crustal structure in seismic wave propagation modelling at continental scale or to compute linearized crustal corrections in continental scale seismic tomography, gravity studies, dynamic topography and other applications that require a reliable crustal structure. Because of its resolution, our model is not suited for local-scale studies, such as the computation of earthquake scenarios, where more detailed knowledge of the structure is required. We plan to update the model as new data will become available, and possibly improve its resolution for selected areas in the future.

Key words: Crustal structure; Europe.

Model download (version Feb 2011):

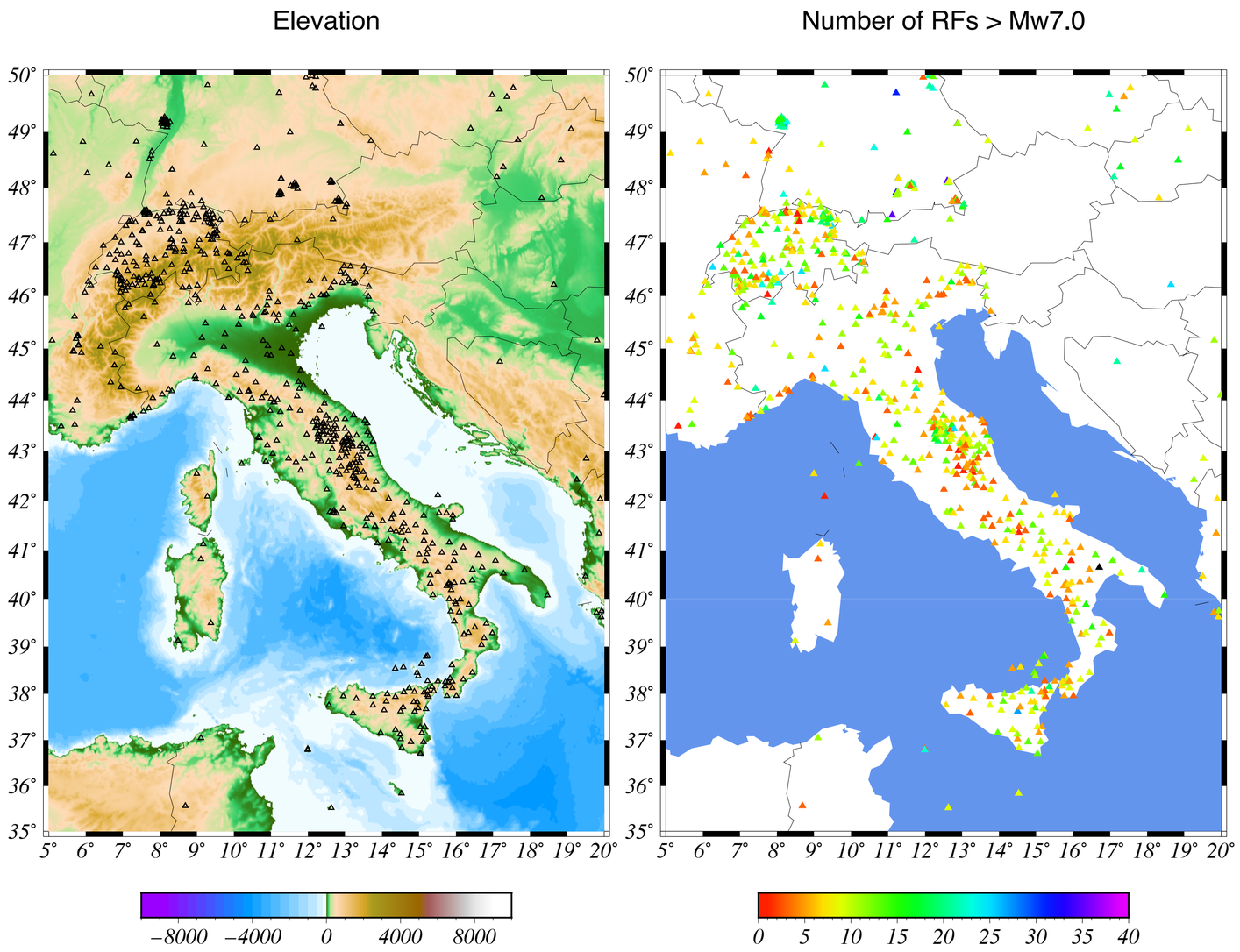
http://eurorem.bo.ingv.it/EPcrust_solar/



Ongoing work by Weisen Shen and colleagues (Stony Brook University)

Good news:

Many stations in Italy.



Slide by Weisen Shen from our online weekly geoneutrino meeting

What else?

Improving global prediction models

Wipperfurth et al. 2020 doi:10.1029/2019JB018433

JGR Solid Earth

RESEARCH ARTICLE
10.1029/2019JB018433

Reference Models for Lithospheric Geoneutrino Signal

S. A. Wipperfurth[1], O. Šrámek[2], and W. F. McDonough[1,3]

[1]Department of Geology, University of Maryland, College Park, MD, USA, [2]Department of Geophysics, Faculty of Mathematics and Physics, Charles University, Prague, Czech Republic, [3]Department of Earth Sciences and Research Center for Neutrino Science, Tohoku University, Sendai, Japan

Key Points:
- Updated geoneutrino emission model compares results using CRUST2.0, CRUST1.0, and LITHO1.0 geophysical models
- Observed differences between geoneutrino signals from different geophysical models is negligible
- Necessary improvements to geoneutrino modeling are identified

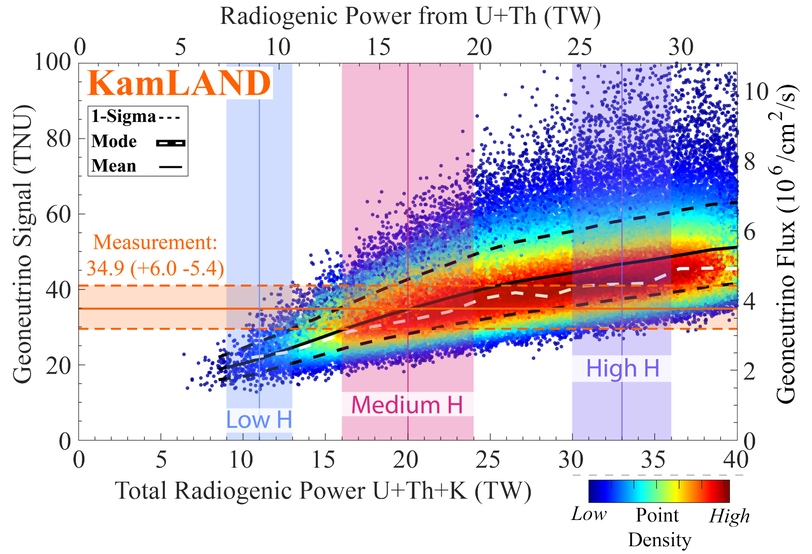
Supporting Information:
- Supporting Information S1

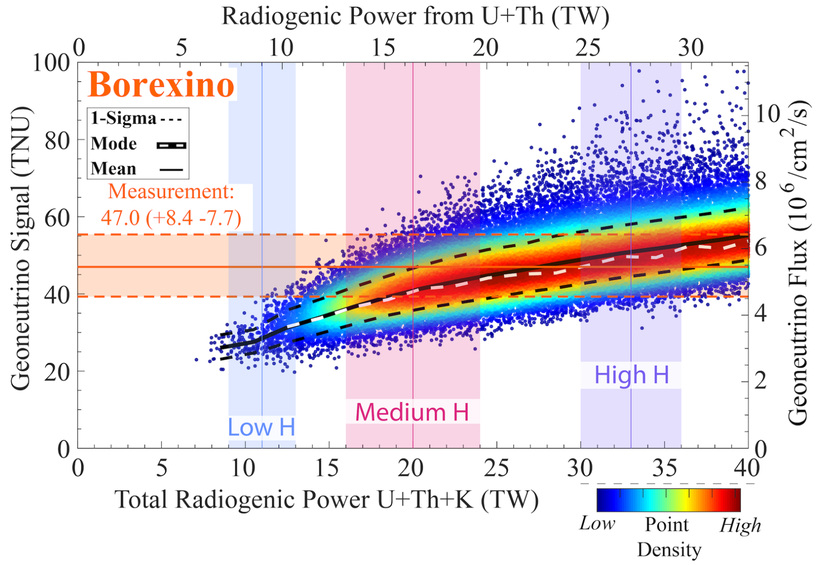
Correspondence to:
S. A. Wipperfurth,
swipp@terpmail.umd.edu

Citation:
Wipperfurth, S. A., Šrámek, O., & McDonough, W. F. (2020). Reference models for lithospheric geoneutrino signal. *Journal of Geophysical Research: Solid Earth*, *125*, e2019JB018433. https://doi.org/10.1029/2019JB018433

Received 24 JUL 2019
Accepted 23 JAN 2020

Abstract Debate continues on the amount and distribution of radioactive heat producing elements (i.e., U, Th, and K) in the Earth, with estimates for mantle heat production varying by an order of magnitude. Constraints on the bulk-silicate Earth's (BSE) radiogenic power also places constraints on overall BSE composition. Geoneutrino detection is a direct measure of the Earth's decay rate of Th and U. The geoneutrino signal has contributions from the local (~40%) and global (~35%) continental lithosphere and the underlying inaccessible mantle (~25%). Geophysical models are combined with geochemical data sets to predict the geoneutrino signal at current and future geoneutrino detectors. We propagated uncertainties, both chemical and physical, through Monte Carlo methods. Estimated total signal uncertainties are on the order of ~20%, proportionally with geophysical and geochemical inputs contributing ~30% and ~70%, respectively. We find that estimated signals, calculated using CRUST2.0, CRUST1.0, and LITHO1.0, are within physical uncertainty of each other, suggesting that the choice of underlying geophysical model will not change results significantly, but will shift the central value by up to ~15%. Similarly, we see no significant difference between calculated layer abundances and bulk crustal heat production when using these geophysical models. The bulk crustal heat production is calculated as 7 ± 2 TW, which includes an increase of 1 TW in uncertainty relative to previous studies. Combination of our predicted lithospheric signal with measured signals yield an estimated BSE heat production of 21.5 ± 10.4 TW. Future improvements, including uncertainty attribution and near-field modeling, are discussed.

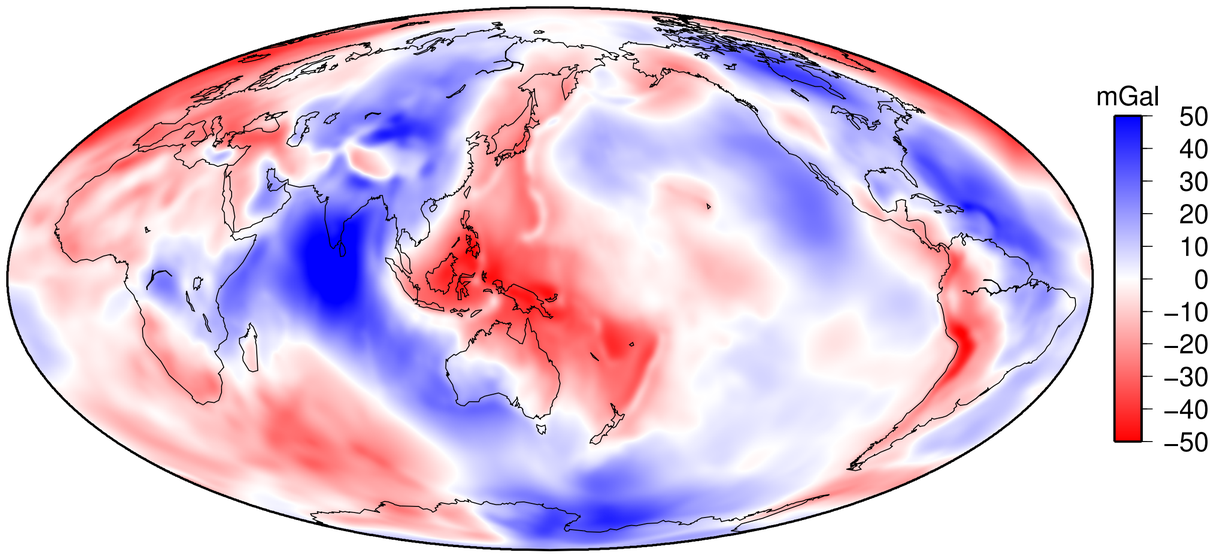




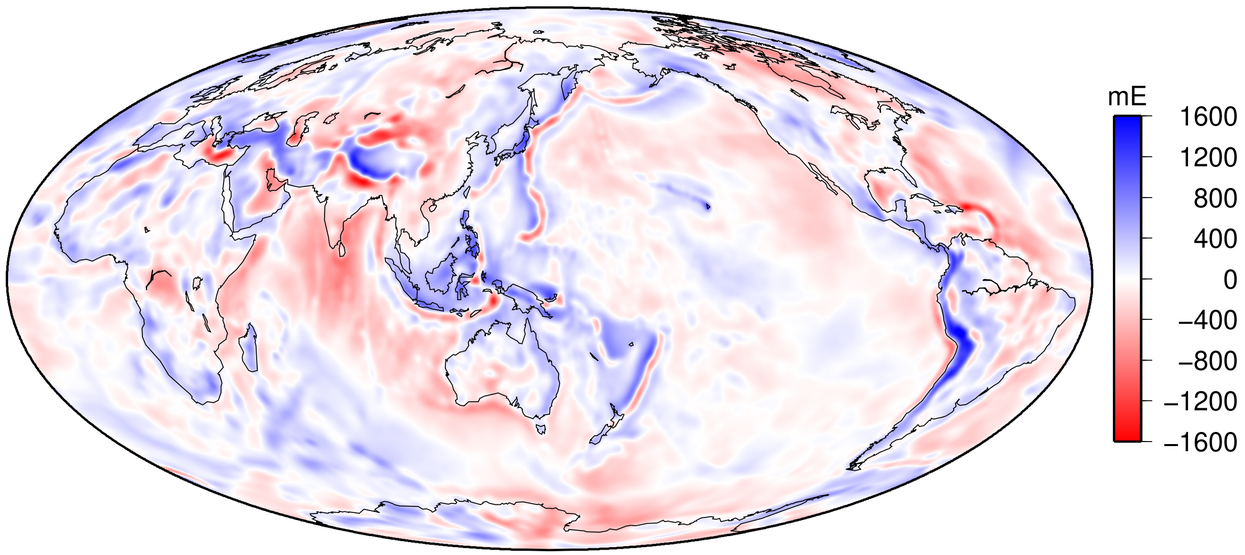
Validation of global crustal model using gravity measurements

Bachelor thesis project of Jaroslav Jaroš (in progress)

T_r GOCE



T_{rr} GOCE



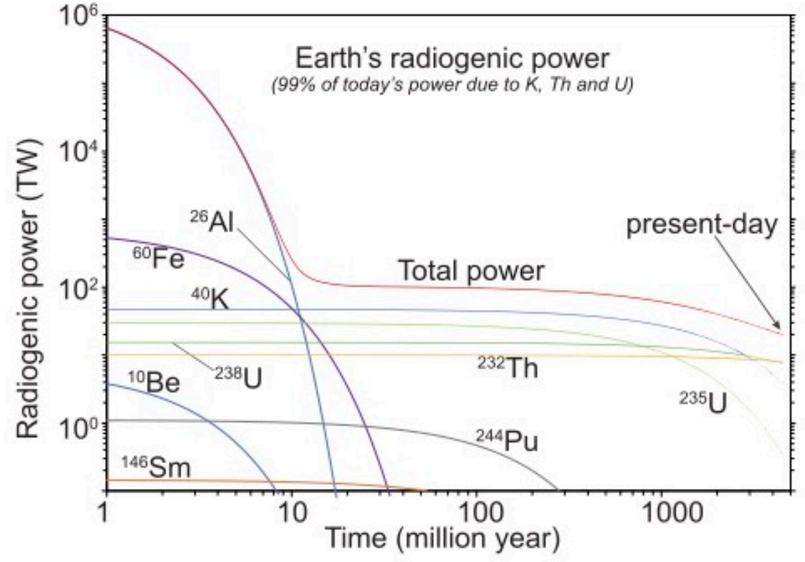
Radiogenic power and geoneutrino flux through time

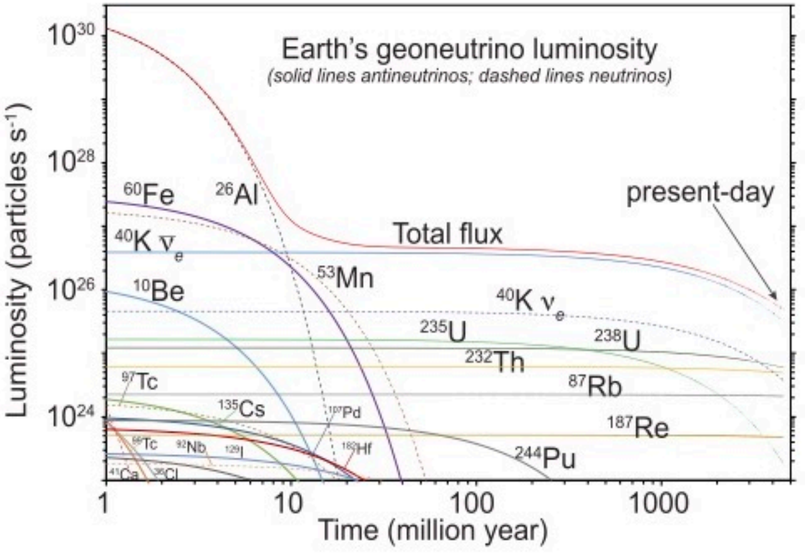
McDonough et al. 2020 doi:10.1029/2019GC008865

Table 4
Short-lived radioactive decay systems in the Earth

Decay system	Decay mode	Shape factor $S(p,q)$	Q (MeV)	Q_h (MeV)	$t_{1/2}$ [a]	$(\widetilde{h}/A)$ [nW/kg-elem] at t_{zero} (CAI)	Mole fraction (%) parent nuclide	Reference
$^{41}Ca \rightarrow {}^{41}K$	EC	–	0.4217	0	$9.94(15)\times10^{4}$	0	$(^{41}Ca/^{40}Ca)_i$=(4.6±1.0)×10^{-9}	Liu (2017)
$^{99}Tc \rightarrow {}^{99}Ru$	β^-	$0.54p^2+q^2$ (M15)	0.2975	0.0957	$2.111(12)\times10^{5}$	46.71	$(^{99}Tc/^{100}Ru)_i$=<3.9×10^{-5}	Wasserburg et al. (1994)
$^{81}Kr \rightarrow {}^{81}Br$	EC	–	0.2809	0.0008	$2.29(11)\times10^{5}$	–	*not available*	–
$^{126}Sn \rightarrow {}^{126}Te$	β^-, β^-	1[b], NuDat[b]	4.0502	2.8597	$2.35(7)\times10^{5}$	3.773×10^{4}	$(^{126}Sn/^{124}Sn)_i$=<3×10^{-6}	Brennecka et al. (2017)
$^{36}Cl \rightarrow {}^{36}Ar$	β^- (98.1%)	M15	0.7095	0.3343	$3.01(2)\times10^{5}$	0.9557	$(^{36}Cl/^{35}Cl)_i$=(1.9±0.3)×10^{-8}	Turner et al. (2013)
$^{36}Cl \rightarrow {}^{36}S$	ε (1.9%)	NuDat[b]	1.1421[EC]	1.5×10^{-4}	$3.01(2)\times10^{5}$	4.291×10^{-4}	"	"
$^{79}Se \rightarrow {}^{79}Br$	β^-	p^2+q^2 [th.]	0.1506	0.0559	$3.26(28)\times10^{5}$	–	*not available*	–
$^{26}Al \rightarrow {}^{26}Mg$	EC (18.3%)	–	4.0044	0.3610	λ_{EC}/λ=0.1827	2057		
$^{26}Al \rightarrow {}^{26}Mg$	β^+ (81.7%)	$p^4+\frac{10}{3}p^2q^2+q^4$ [th.]	2.9824	2.7593	$\lambda_{\beta^+}/\lambda = 0.8173$	1.572×10^{4}		
$^{26}Al \rightarrow {}^{26}Mg$	Overall			3.1203	$7.17(24)\times10^{5}$	1.777×10^{4}	$(^{26}Al/^{27}Al)_i = (5.25\pm0.02)\times10^{-5}$	Larsen et al. (2011)
$^{10}Be \rightarrow {}^{10}B$	β^-	$p^4+\frac{10}{3}p^2q^2+q^4$ [th.]	0.5568	0.2527	$1.387(12)\times10^{6}$	2.270×10^{4}	$(^{10}Be/^{9}Be)_i$=(5.3±0.5)×10^{-4}	Liu et al. (2010)
$^{93}Zr \rightarrow {}^{93}Nb$	β^-	p^2+q^2 [th.]	0.0903	0.0456	$1.61(5)\times10^{6}$	–	*not available*	–
$^{150}Gd \rightarrow {}^{146}Sm$	α	–	2.8077	2.8077	$1.79(8)\times10^{6}$	–	*not available*	–
$^{135}Cs \rightarrow {}^{135}Ba$	β^-	$0.10p^2+q^2$ (M15)	0.2688	0.0615	$2.3(3)\times10^{6}$	119.4	$(^{135}Cs/^{133}Cs)_i$~2.8 ×10^{-4}	Bermingham et al. (2014)
$^{60}Fe \rightarrow {}^{60}Ni$	β^-, β^-	1[b], NuDat[b]	3.0598	2.7077	$2.62(4)\times10^{6}$	0.3635	$(^{60}Fe/^{56}Fe)_i = (1.01\pm0.14)\times10^{-8}$	Tang and Dauphas (2015)
$^{154}Dy \rightarrow {}^{150}Gd$	α	–	2.9451	2.9451	$3.0(15)\times10^{6}$	–	*not available*	–
$^{53}Mn \rightarrow {}^{53}Cr$	EC	–	0.5968	0	$3.74(4)\times10^{6}$	0	$(^{53}Mn/^{55}Mn)_i = (6.28\pm0.33)\times10^{-6}$	Trinquier et al. (2008)
$^{98}Tc \rightarrow {}^{98}Ru$	β^-	1[b]	1.794	1.5165	$4.2(3)\times10^{6}$	212.4	$(^{98}Tc/^{96}Ru)_i$~2×10^{-5}	Becker and Walker (2003)
$^{97}Tc \rightarrow {}^{97}Mo$	EC	–	0.3247	0	$4.21(16)\times10^{6}$	0	$(^{97}Tc/^{98}Ru)_i$=<4×10^{-4}	Dauphas et al. (2003)
$^{107}Pd \rightarrow {}^{107}Ag$	β^-	p^2+q^2 [th.]	0.0341	0.0133	$6.5(3)\times10^{6}$	0.2768	$(^{107}Pd/^{108}Pd)_i$=(3.5±0.05)×10^{-5}	Matthes et al. (2018)
$^{182}Hf \rightarrow {}^{182}W$	β^-, β^-	p^2+q^2 [th.], NuDat[b]	2.1958	1.8276	$8.90(9)\times10^{6}$	87.07	$(^{182}Hf/^{180}Hf)_i = (1.018\pm0.022)\times10^{-4}$	Kruijer et al. (2014)
$^{129}I \rightarrow {}^{129}Xe$	β^-	$p^2+3.16q^2$ (M15)	0.1889	0.0853	$1.57(4)\times10^{7}$	12.71	$(^{129}I/^{127}I)_i$~1.4×10^{-4}	Gilmour and Crowther (2017)
$^{205}Pb \rightarrow {}^{205}Tl$	EC	–	0.05067	0	$1.73(7)\times10^{7}$	0	$(^{205}Pb/^{204}Pb)_i$=(1.0±0.2)×10^{-3}	Baker et al. (2010)
$^{92}Nb \rightarrow {}^{92}Zr$	EC	–	2.0059	1.4956	$3.47(24)\times10^{7}$	16.71	$(^{92}Nb/^{93}Nb)_i$=(1.7±0.3)×10^{-5}	Iizuka et al. (2016)
$^{244}Pu \rightarrow {}^{232}Th$	3α, 2β^- [c]	NuDat[b]	17.0836	15.6264	$8.11(3)\times10^{7}$	1.363×10^{4}	$(^{244}Pu/^{238}U)_i$ ~0.0079	Turner et al. (2007)
$^{146}Sm \rightarrow {}^{142}Nd$	α	–	2.5288	2.5288	$1.03(5)\times10^{8}$	87.96	$(^{146}Sm/^{144}Sm)_i$ = (8.28±0.22)×10^{-3}	(Marks et al., 2014; Meissner et al., 1987)

Note. Q is the energy of transition (Q value) not accounting for possible branching; Q_h is the energy that remains in the Earth to provide radiogenic heating per decay, accounting for branching. M15 = shape factor from Mougeot (2015). [EC]Reports the Q value of EC branch.
[a]Half-lives are from NNDC (www.nndc.bnl.gov). Heating coefficients $(\widetilde{h}/A)$ (in nW kg-elem^{-1}), so that radiogenic power per unit mass of rock $\widetilde{h}$ can be calculated from $\widetilde{h} = (\widetilde{h}/A) \times A$, A being the elemental mass fraction (kg-element/kg-rock), are obtained similarly to Equation 7. (Note that we report here $(\widetilde{h}/A)$ in nW (c.f., (7), which is given in μW) for these SLR.) [b]In some cases, we use shape factors equal to 1 or NuDat-tabulated mean electron energies for forbidden transitions, due to lack of better inputs. [c]^{244}Pu also undergoes spontaneous fission to $^{130-136}$Xe isotopes with a fission branching probability of 0.12%. The individual decay energies for the double β^- steps are as follows: $^{126}Sn \rightarrow {}^{126}Te$: Q=0.3782+3.6720=4.0502 MeV; $^{60}Fe \rightarrow {}^{60}Ni$: Q=0.237+2.8228=3.0598 MeV; $^{182}Hf \rightarrow {}^{182}W$: Q=0.3813+1.8145=2.1958 MeV. The individual decay energies for $^{244}Pu \rightarrow {}^{232}Th$: Q=4.6655+0.3991+2.1901+5.2558+4.5731=17.0836 MeV. Uncertainties cited in the initial ratios of the short-lived nuclides are 1 standard deviation.





Making (pre-)life

THE JOURNAL OF PHYSICAL CHEMISTRY B

Pastorek et al. 2020 doi:10.1021/acs.jpcb.0c05233

pubs.acs.org/JPCB Article

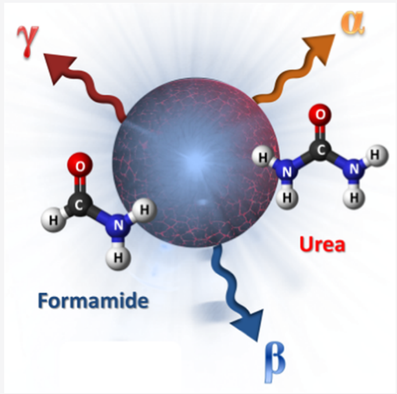
Primordial Radioactivity and Prebiotic Chemical Evolution: Effect of γ Radiation on Formamide-Based Synthesis

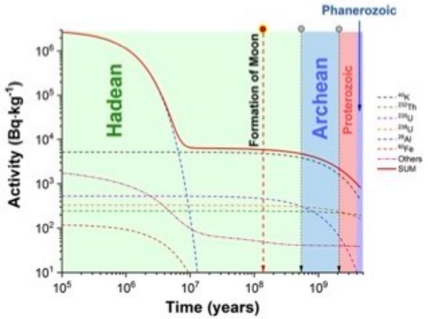
Adam Pastorek, Martin Ferus, Václav Čuba, Ondřej Šrámek, Ondřej Ivanek, and Svatopluk Civiš*

Cite This: *J. Phys. Chem. B* 2020, 124, 8951–8959 Read Online

ACCESS | Metrics & More | Article Recommendations | Supporting Information

ABSTRACT: Although the effect of ionizing radiation on prebiotic chemistry is often overlooked, primordial natural radioactivity might have been an important source of energy for various chemical transformations. Estimates of the abundances of short-lived radionuclides on early Earth suggest that the primordial intensity of endogenous terrestrial radioactivity was up to 4×10^3 times higher than it is today. Therefore, we assume that chemical substances in contact with radioactive rocks should therefore undergo radiolysis. The calculations are followed by research investigating the influence of ionizing γ radiation on basic prebiotic substances, including formamide mixed with various clays, which might have played the role of a catalyst and an agent that partially blocked radiation that was potentially destructive for the products. Our explorations of this effect have shown that the irradiation of formamide–clay mixtures at doses of ~6 kGy produces significant amounts of urea (up to the maximal concentration of approximately 250 mg L^{-1}), which plays a role in HCN-based prebiotic chemistry.

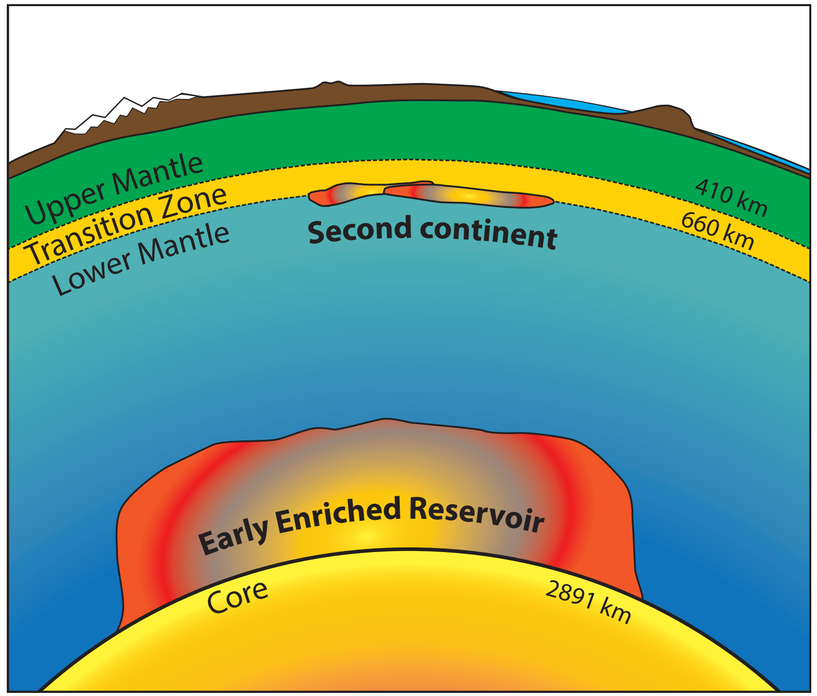


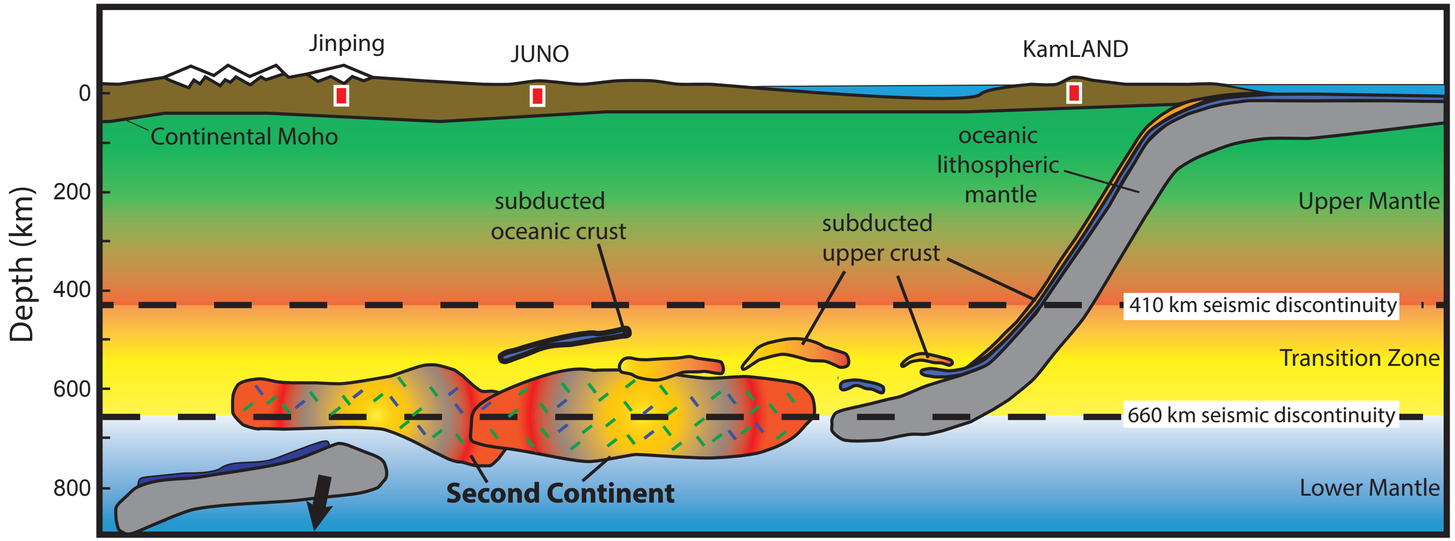


Imaging Geochemical Anomalies in the Mantle Using Geoneutrinos

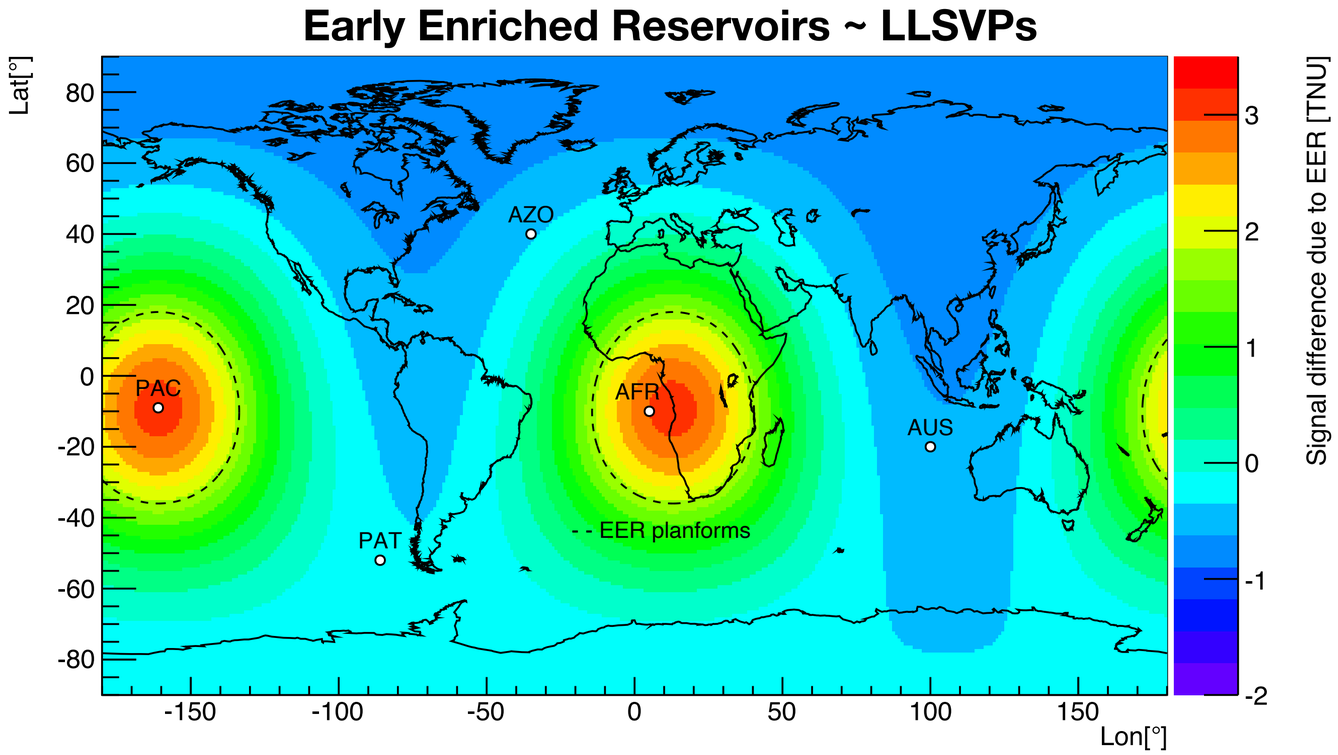
Roskovec et al., submitted to G^3

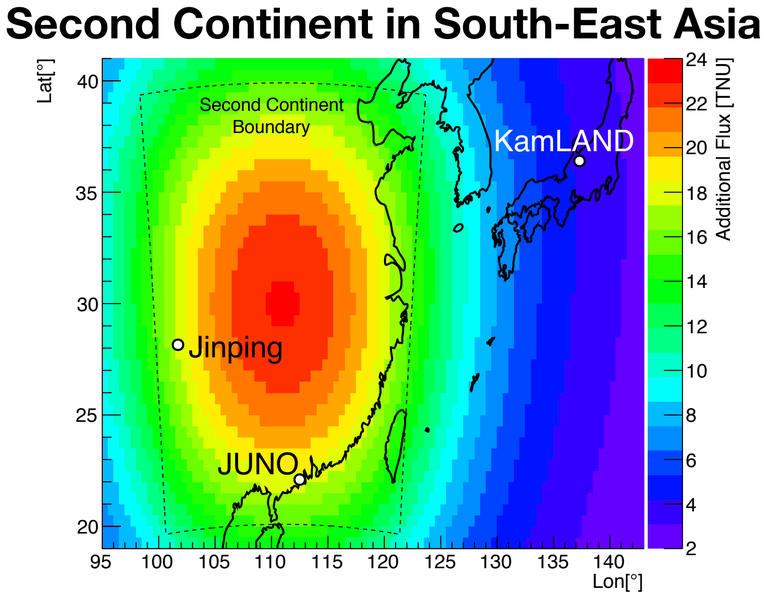
- **Second Continent:** Material of Upper Continental Crust entrained and subducted in oceanic plate subduction setting, accumulated at the base of the Transition Zone.
- **Early Enriched Reservoir:** Material of early formed crust, recycled into the mantle where it sank near the core–mantle boundary and remained since.

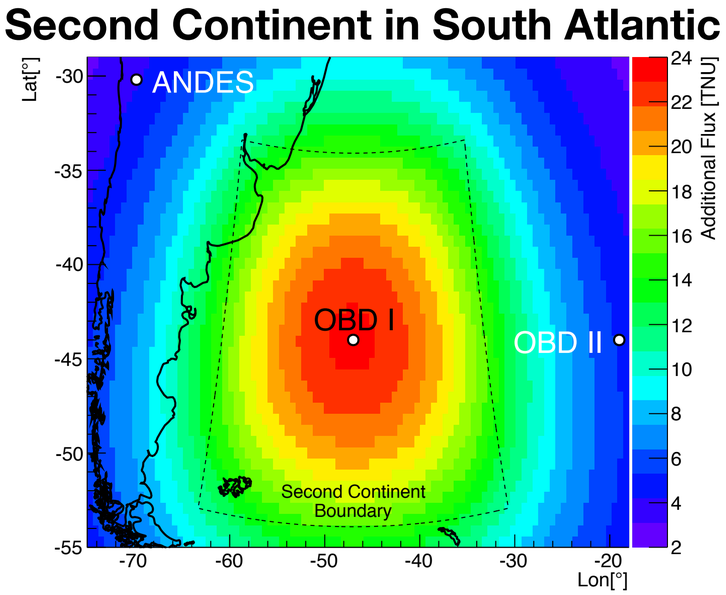




Could we image these anomalies?



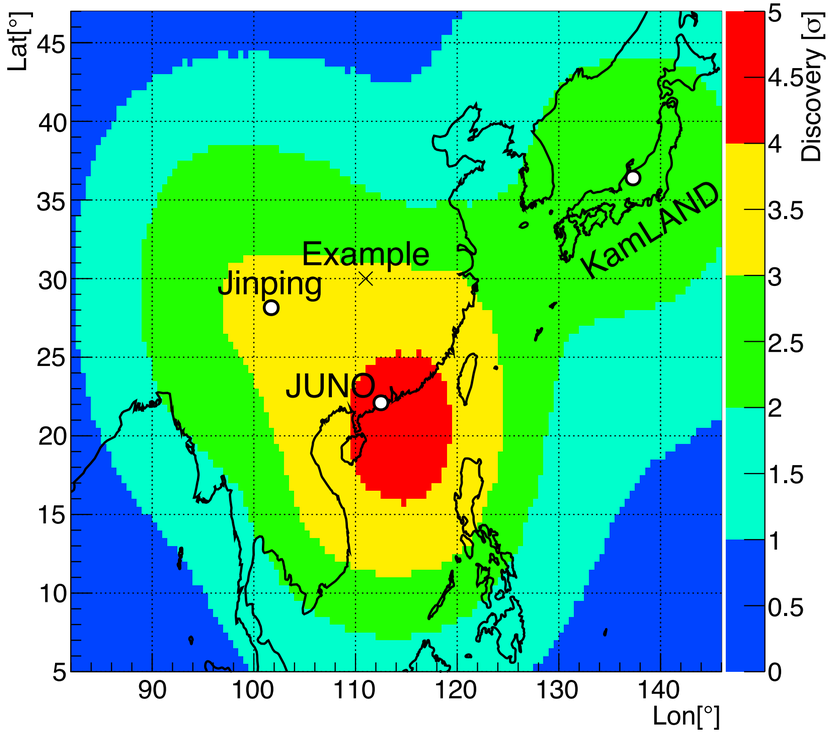


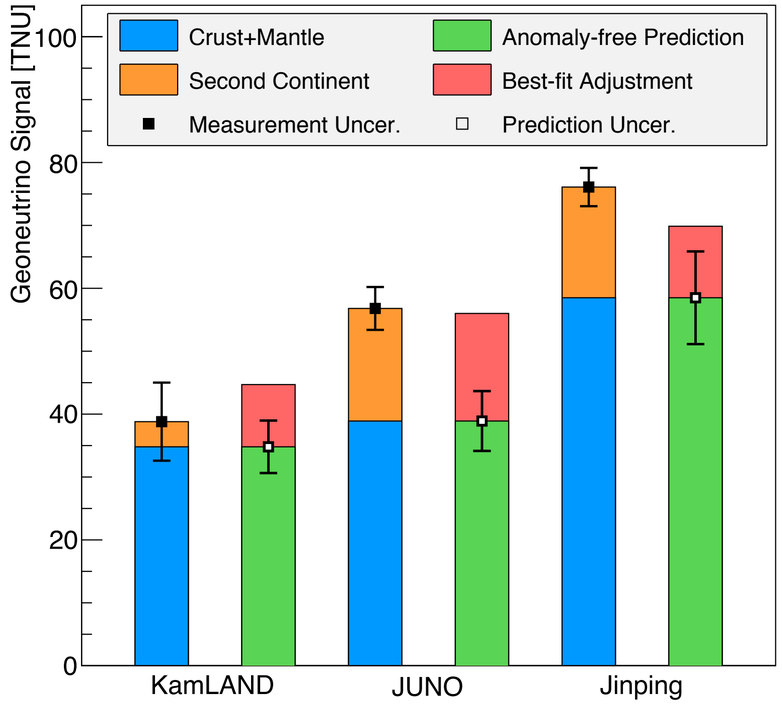


Quantifying the Second Continent discovery potential in South-East Asia

$$\chi^2_{min} = \min_{\alpha's} \sum_{i=1,2,3}^{exp.} \frac{\left(\overline{T}_i + S_i - (\overline{T}_i + \alpha_i \sigma_i)\right)^2}{\sigma^2_{m,i}} + \alpha^T M^{-1}_{cor} \alpha$$

$\sqrt{\chi^2_{min}}$ = discovery potential in units of σ



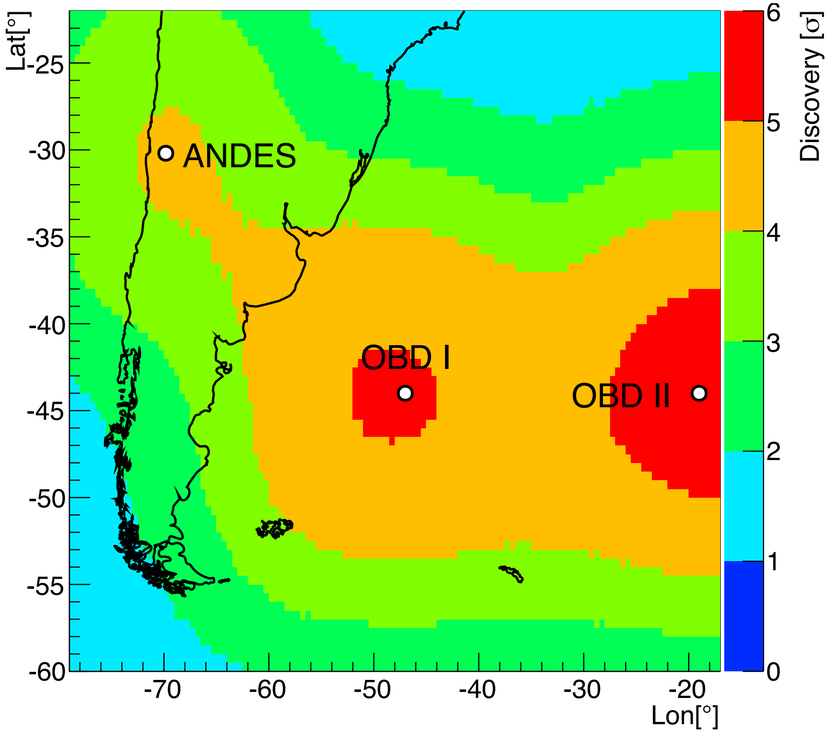


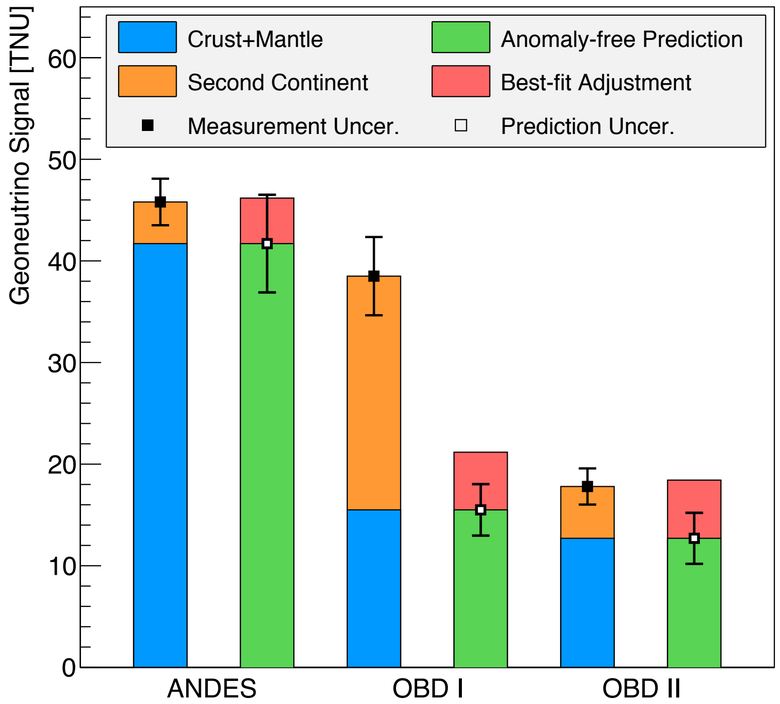
Second Continent discovery potential in South Atlantic

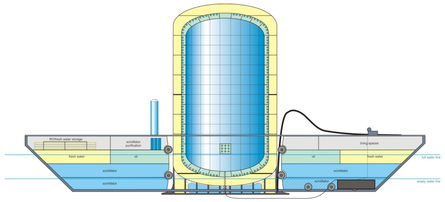
OBD = Ocean Bottom Detector

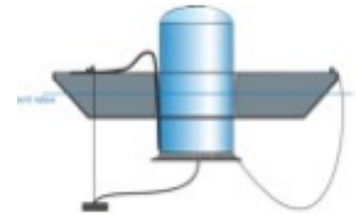
$$\chi^2_{min} = \min_{\alpha} \sum_{i=1,..,5}^{\text{exp.}} \frac{\left(\overline{T}_i + E_i - (\overline{T}_i + \alpha\sigma_i)\right)^2}{\sigma^2_{m,i}} + \alpha^2$$

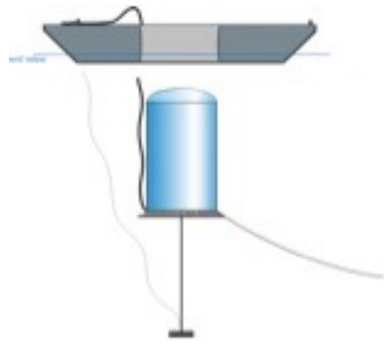
$\sqrt{\chi^2_{min}}$ = discovery potential in units of σ

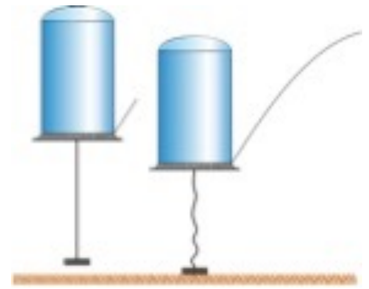






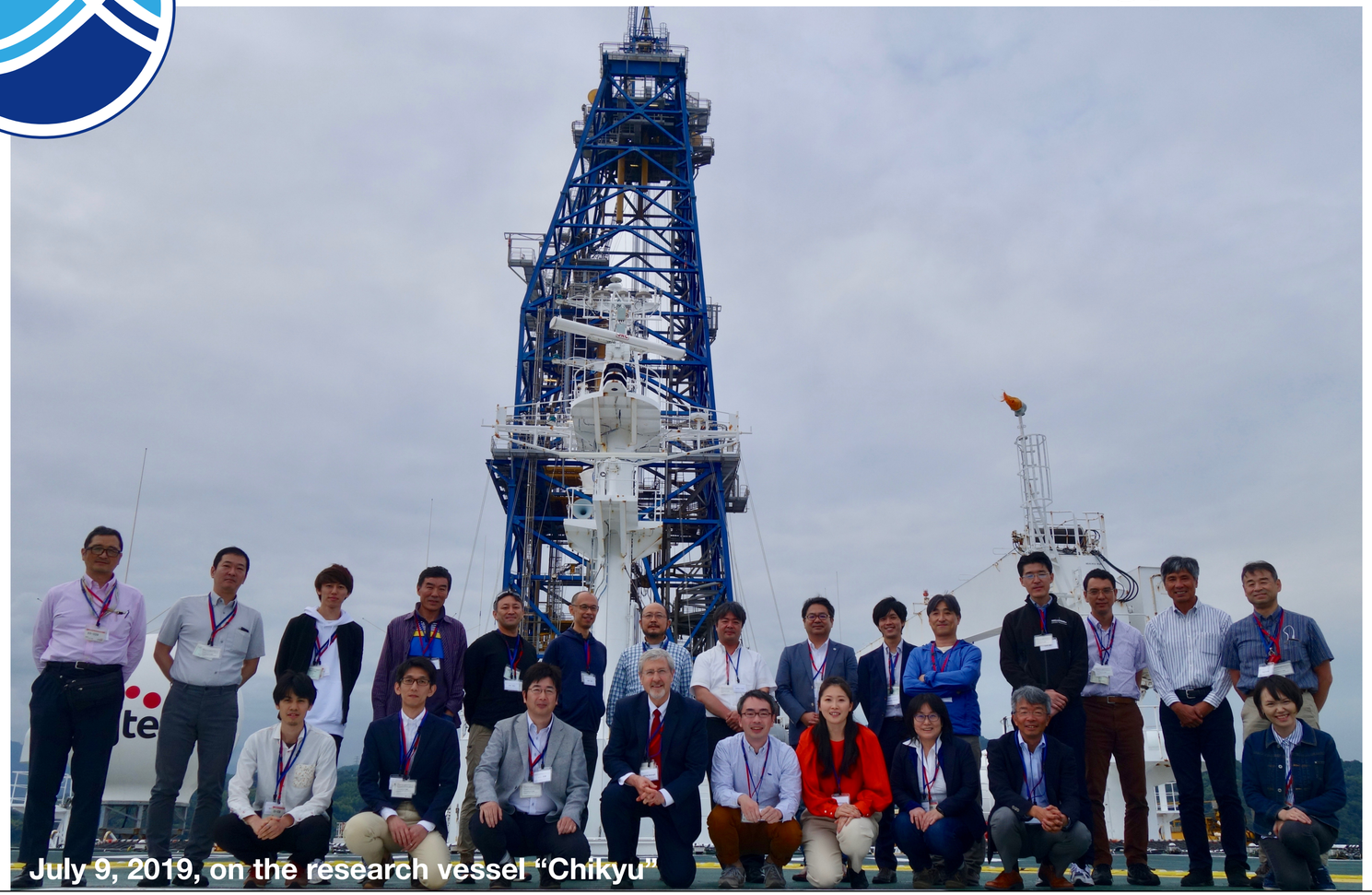






In 2019, Members of JAMSTEC and Tohoku University established a joint working group for OBD

JAMSTEC: Japan Agency for Marine-Earth Science and Technology

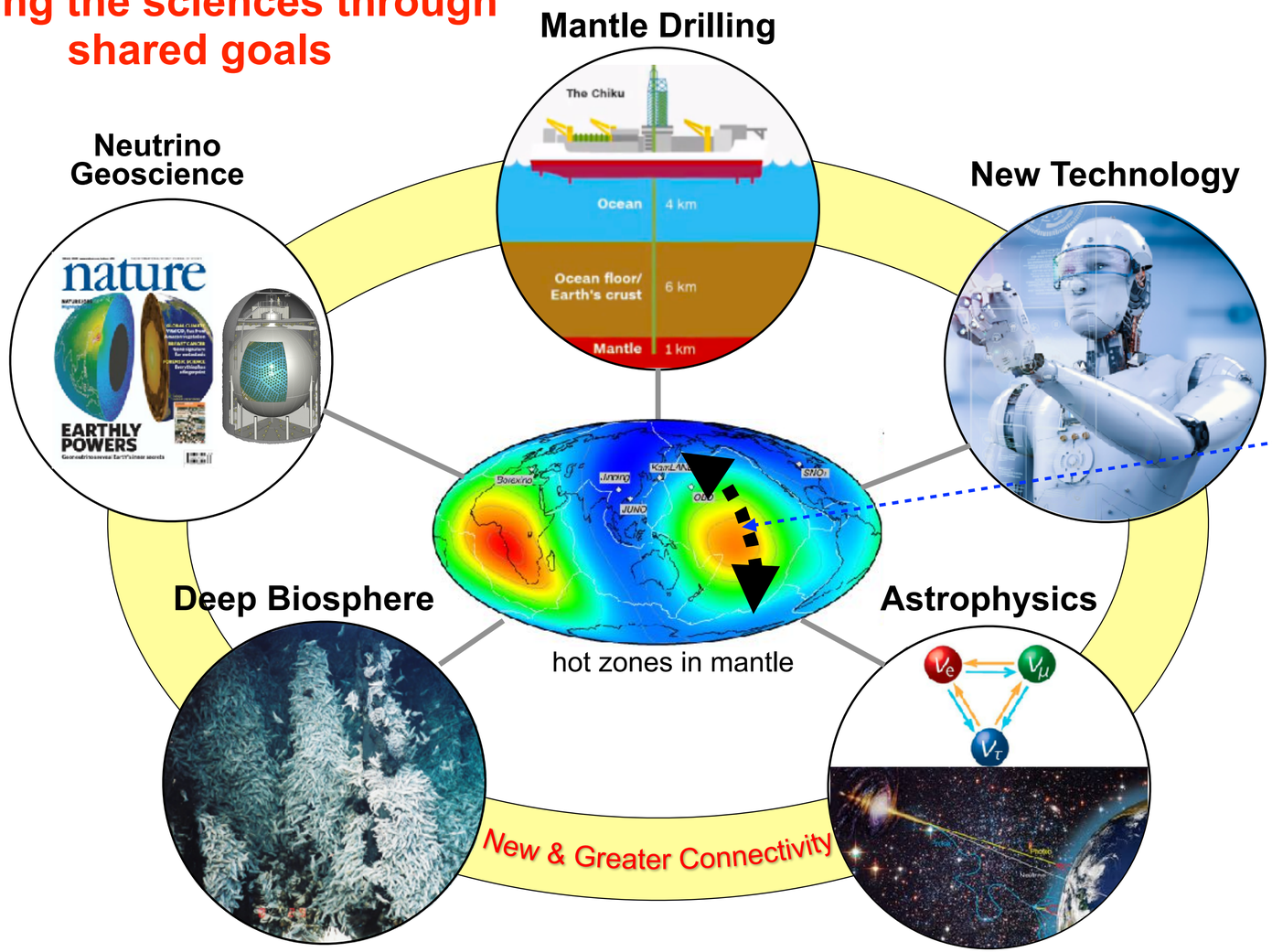


July 9, 2019, on the research vessel "Chikyu"

Slide from Hiroko Watanabe and Kenta Ueki at Neutrino Geoscience 2019 Prague

Goal of Our Program

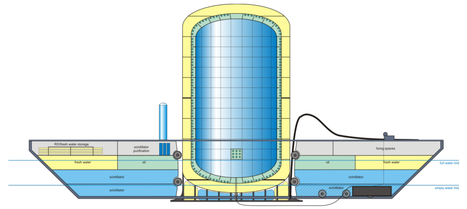
Linking the sciences through shared goals



Our Tool

mature science and technology

Geoneutrino detector in the ocean
(Ocean Bottom Detector)

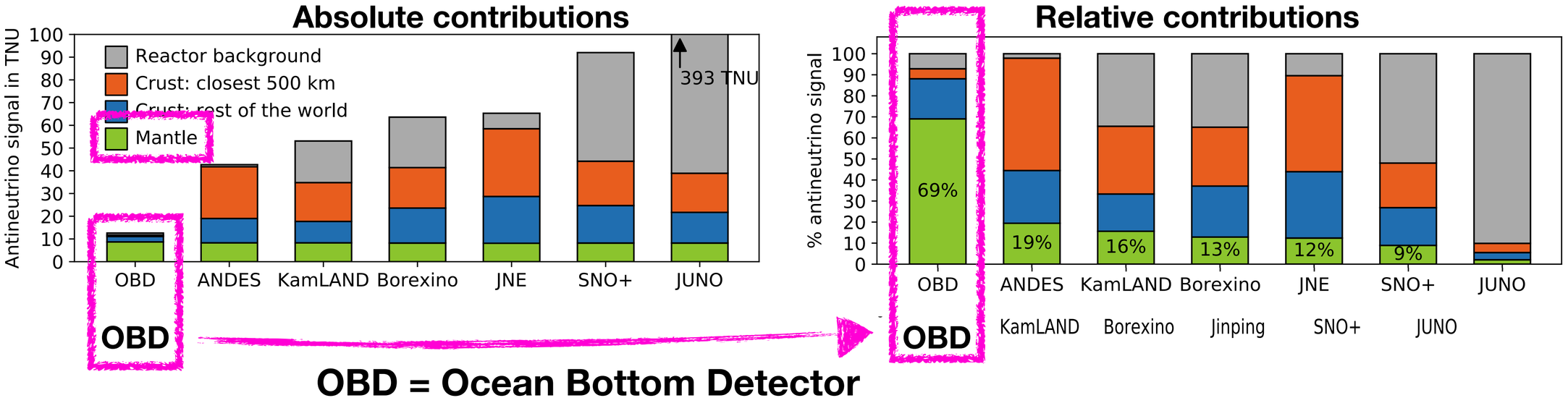


- Mapping hidden features in the mantle using breakthrough technology
- Interdisciplinary collaboration between physics, geoscience and engineering
- Revealing unknown unknowns

Program Goal **Create new & greater connectivity between independent fields**

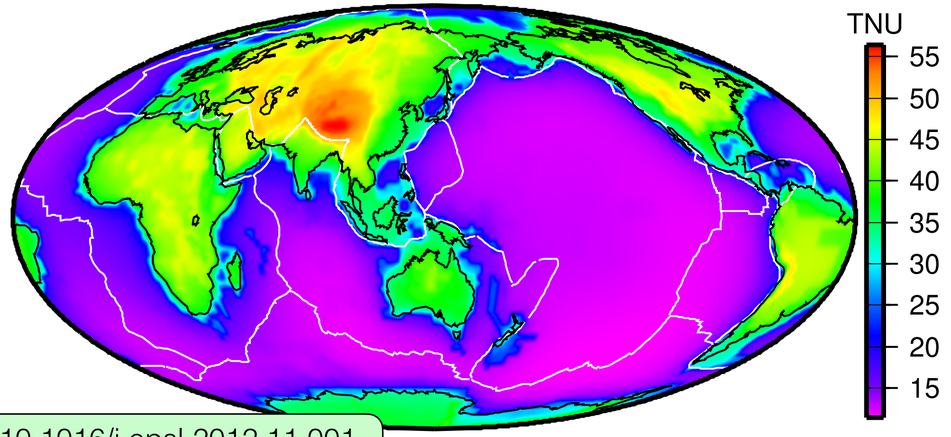
Slide from Hiroko Watanabe (December 2020)

OBD: Measure in the ocean

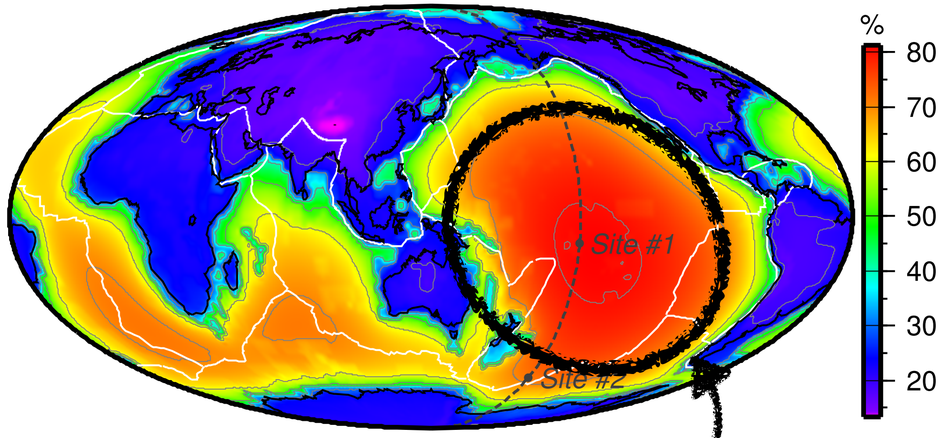


OBD = Ocean Bottom Detector

Crust + mantle (TNU)



Mantle contribution to total signal (%)



Šrámek et al 2013 doi:10.1016/j.epsl.2012.11.001

Here is where we want to measure the mantle

Challenges of geoneutrino research

- Split measured value into two contributions
- Super difficult at continental sites
  – Currently measuring experiments (two) and being constructed (three more)
- Easy with an ocean bottom detector
  – “Ocean Bottom Kamland”…?
- The traditional wishlist:
  – directional measurement
  – measuring ^{40}K neutrinos